ABSTRACT

THE L-AUGER SPECTRUM OF In^{113} AS DERIVED FROM THE ELECTRON CAPTURE DECAY OF SN^{113}

by Raymond J. Kriščiokaitis

The low energy range of the M.S.U. 11 12 iron-free beta-ray spectrometer has been extended down to 1 kev by means of electrostatic post-focusing acceleration of the electron beam. It has been shown that accurate relative intensity measurements of electron spectra are possible at least down to these energies.

The spectrometer data acquisition system has been automated to facilitate more reliable and efficient data taking particularly as this applies to weak low energy Auger spectra.

The L-Auger spectrum of In^{113} as derived from the electron capture decay of Sn^{113} (~2 to 4 kev) has been measured and the major Auger lines and groups identified. Order of magnitude of the relative intensities of these lines has also been determined. The effective incremental charge ΔZ has been determined for the most prominent and important transitions. $\Delta Z = 0.55$; 0.67 for transitions of the type $L_{1,2,3}\text{-}M_{1,2,3}M_{1,2,3}$; $L_{1,2,3}\text{-}M_{4,5}M_{4,5}$, respectively.

It has been shown that the spectrum exibited intermediate coupling features and that shifts of Auger lines due to double vacancy effects probably exist.

THE L-AUGER SPECTRUM OF IN-113 AS DERIVED FROM THE ELECTRON CAPTURE DECAY OF SN-113

By

Raymond J. Kriščiokaitis

A THESIS

Submitted to
Michigan State University
in partial fulfillment of the requirements
for the degree of

DOCTOR OF PHILOSOPHY

Department of Physics and Astronomy

1965

ACKNOWLEDGEMENT

I would like to express my deepest appreciation to Professor Sherwood K. Haynes for providing me the opportunity to carry out this investigation and for giving me invaluable guidance throughout the course of the problem.

Professor William H. Kelly has been a kind and helpful adviser during the period of Professor Sherwood K. Haynes absence. Many thanks to him.

Professor Hugh McManus has given me important perspective concerning some theoretical aspects of the Auger process. I express my gratitude for this.

I am grateful also to the men in the electronics and machine shops for their aid during the construction phases of the problem.

Other people to whom I wish to express my gratitude are Robert Francoise and George Flemming, who eagerly assisted in various ways in the preparation of the thesis, Jerry Lerner, who was in charge of the isotopic mass separator at Argonne and Argonne National Laboratory for the use of the separator.

TABLE OF CONTENTS

[redacted]

TH

LIST OF TABLES

LIST OF FIGURES

[redacted]

TH

CHAPTER 1

INTRODUCTION

Contemporary experimental investigations of nuclear structure and nuclear forces consist of a vast array of techniques and methods represented by a variety of instruments. It is generally found that no one technique or method will monopolize an area of investigation, for it will either be displaced by a new and an improved method, with greater probing power, or will be forced to refine itself, and thus continue in its usefulness by complementing its competitor. The underlying premise for success of such a pattern of development is that the scientist must respond to the challenge and stimulus provided by new discoveries, both in the theoretical and experimental areas.

Low energy nuclear physics, more specifically nuclear spectroscopy, has made a quantum jump during the past decade, both in terms of instrumental improvements (e.g., perfection of high resolution electron spectrometers and solid state detectors), and advances in theory (e.g., critical study of the conservation law of parity in weak interactions by Lee and Yang). This is attested in the recent edition of α-β-γ-Ray Spectroscopy by K. Siegbahn[1] which doubles the amount of material in the previous edition.

One of the more recent developments has been the refinement of the theory of orbital electron capture by nuclei as formulated by Bahcall.[2,3,4] Orbital capture theory has been presented by Marshak,[5] Brysk and Rose,[6] Odiot and Daundel,[7] and reviewed by Bouchez and Depommier,[8] and Robinson and Fink.[9] The latter have pointed out a systematic discrepancy between measured L/K electron capture ratios and the predictions of Brysk and Rose.[6] Bahcall's calculations,[2,3,4] which include atomic variables in the initial and final states and take account of exchange and imperfect overlap effects, tend to bring theory and experiment closer together. Besides stimulating the need for more precise measurements of electron capture ratios using the accepted techniques,[8,9] the refined theoretical results warrant the investigation of the usefulness of modern precision spectrometers as tools for such refined measurements.

The M.S.U. iron-free double-focusing $\pi\sqrt{2}$ beta-ray spectrometer[10] seemed to afford an excellent opportunity for this kind of study. It is a precision instrument capable of very high resolution. A detailed account of its characteristics may be found in reference 10.

The global problem, as envisaged at the start, was to be the measurement of the relative orbital capture probability ratio L/K, and possibly $L_1/L_2/L_3$. The key to the measurement was the study of the L-Auger and K-Auger electrons (I. Bergstrom and C. Nordling ref. 1) created

during the deexcitation of the atom, after it has been ionized by the orbital capture process. Noteworthy is the fact, that the Auger process itself has not been thoroughly investigated. The exception is the K-LL Auger group. The other groups, such as the K-LY, K-XY and the L-XY, have been investigated relatively little, both experimentally and theoretically. Thus in effect, the Auger process for the element in question must be studied experimentally and more fully understood and interpreted before Auger spectra can be used in an analysis to obtain the electron relative orbital capture probabilities.

The choice of the specific capture process,[11] $Sn^{113}(119d) \xrightarrow{EC} In^{113m}(1.7h)$, which in turn decays to the ground state of In^{113} with the emmission of a 392 kev gamma and conversion electrons,* was made for the following reasons.

1. The study of the L-Auger spectrum emanating from a medium Z atom had never been attempted previously and our attempt to study such a spectrum involving the difficult problem of detection of low energy electrons was a matter of interest by itself.

2. Additionally, Z = 49 is a good place to search for energy shifts of L-Auger lines due to double

---

*A weak electron capture branch (2%) also feeds a high lying (648 kev) In^{113} state.

[redacted]

THES

vacancies following the K-LL transitions.* The understanding of this effect would be important for any Z if the relative orbital capture ratio such as $L_1/L_2/L_3$ is ever to be measured.

3. The radioactive substance was easy to produce due to a large neutron capture cross section[12] for Sn^{112}, which could be readily obtained possessing an isotopic purity of 72%. Also, Sn^{113} could be easily separated from the stable Sn^{112} and other isotopic contaminants by means of an electromagnetic mass separator, thus fulfilling the need for a high specific activity source.

4. It was found during earlier experiments in this laboratory that separation of trace amounts of In^{113} from Sn^{113} was possible by means of a vacuum evaporation technique using the much higher volatility of Indium to an advantage. This gave us the capability of observing the Auger process separately, due to the vacancies created by the conversion process.

It is inherent in the study of Auger spectra (generally of low intensity) that the experimenter is faced with lengthy running times. For the sake of expediency the data taking procedure of the spectrometer

---

*The K Auger yield (a_K) is substantially higher in this region than for heavy elements (I. Bergstrom and C. Nordling ref. 1).

[redacted]

THES

was automated. This is treated in CH II.

Our choice of the above electron capture process required the extension of the low energy range of the spectrometer down to at least 2 kev by means of post-acceleration of the focused electron beam.* Therefore, a successful post-focusing acceleration cell had to be developed in order to insure reliable electron intensity measurements. It is described in CH III.

The requirement of producing extremely thin sources (several atomic monolayers in depth), needed to avoid source absorption losses and consequent spectral distortion, constituted also another problem that had to be solved.

Chapter IV shows the results of the composite (capture and conversion) L-Auger spectrum of Sn^{113}-In^{113} and constitutes the preliminary attack on the problem of measurement of the relative orbital capture probabilities through the examination of the Auger spectrum by means of a modern high precision electron spectrometer.

---

*The 2 kev figure is the endpoint energy of the L-Auger spectrum for elements with Z~50.

[redacted]

THI

CHAPTER II

AUTOMATIZATION OF THE DATA ACQUISITION SYSTEM

A. Introductory Remarks

It has been said that necessity is the mother of invention. This chapter is an illustration of such a phenomenon.

Peculiar to low transmission instruments such as the $\pi\sqrt{2}$ spectrometer at Michigan State University, is the fact that data collection or acquisition is usually a very long and tedious process requiring running times often counted in units of months. This is particularly true if one confines himself to the study of Auger spectra, which generally are weak in intensity to start with; the gathering of statistics is therefore very time consuming. Once the spectrometer is set in operation it is best to collect data continuously and therefore minimize the rate of equipment breakdown and consequent down-time. Furthermore, when studying short half-life sources, the need for continuous collection of data becomes even more stringent. Typical sampling of momentum is of the order of two to ten minutes per momentum position. This means that, before spectrometer automatization, the momentum step-up or step-down had to be made manually after each counting interval, requiring the operator not only to change the momentum value by turning the knobs on the

TH

decade voltage divider,[10] but also to reset the counting cycle. Needless to say, then, automatization of such a system was desirable, not only from the standpoint of doing good physics, but also from the standpoint of convenience and the saving of the costs of manual labor.

The approach to this problem was one of an inventor rather than of an electrical engineer. The heart of the design is a multistation electromechanical rotary switch.* It is powered by a direct current rotary solenoid** which is coupled to an output shaft through a floating ratchet mechanism. The shaft drives the rotors of a series of wafer switches*** which may be programmed to perform multiple switching functions. A set of four of these rotary switches is mechanically coupled to the lower four decade units. By a programming process utilizing the wafers to drive the decade divider (or step up the momentum or magnetic field) systematically at predetermined intervals, one may sweep the momentum region of interest at preset time intervals.

A workable model was constructed and operated for 500 hours during the RaD L Auger run.[13] It was later discovered that what appears to be a similar design was already in operation at Uppsala[14] with a magnetic spec-

---

*Ledex Inc., Dayton, Ohio.

**Size 5S awg. no. 26 (no interrupter).

***1-pole 12-throw W-548 (phen.).

[redacted]

THE

trometer for neutron capture experiments.

The present system is modest in terms of the data acquisition and data handling systems that are in vogue at many larger laboratories. The ground work for a more sophisticated arrangement has been laid, however, and the basic circuits of the present system can be easily extended to a more versatile automatic operation of the spectrometer.

B. Design and Operation

Figure 1A illustrates the basic elements of the automatized system. For automatic operation the timer* is set to count for a desired time interval, and the starting momentum position is set manually by adjusting the decade divider. The intervals at which the momentum region of interest is to be swept are programmed on the program deck. When the scaler count switch is thrown, counter pulses start accumulating until the preset counting time interval elapses. Any time during this first counting interval for the starting momentum position the power switch connecting the d.c. supply (0-36 v) to the pulser may be thrown (switch S_4 fig. 2).**

---

*Eagle Signal Corp., Moline, Ill.

**Switches S_0, S_1, S_2, S_3, remain normally closed for automatic operation. They were primarily installed for testing isolated operation of individual solenoids.

[redacted]

THES

Figure 1. (A) Schematic Representation of Automated Data Acquisition System.

(B) Power Flow Diagram.

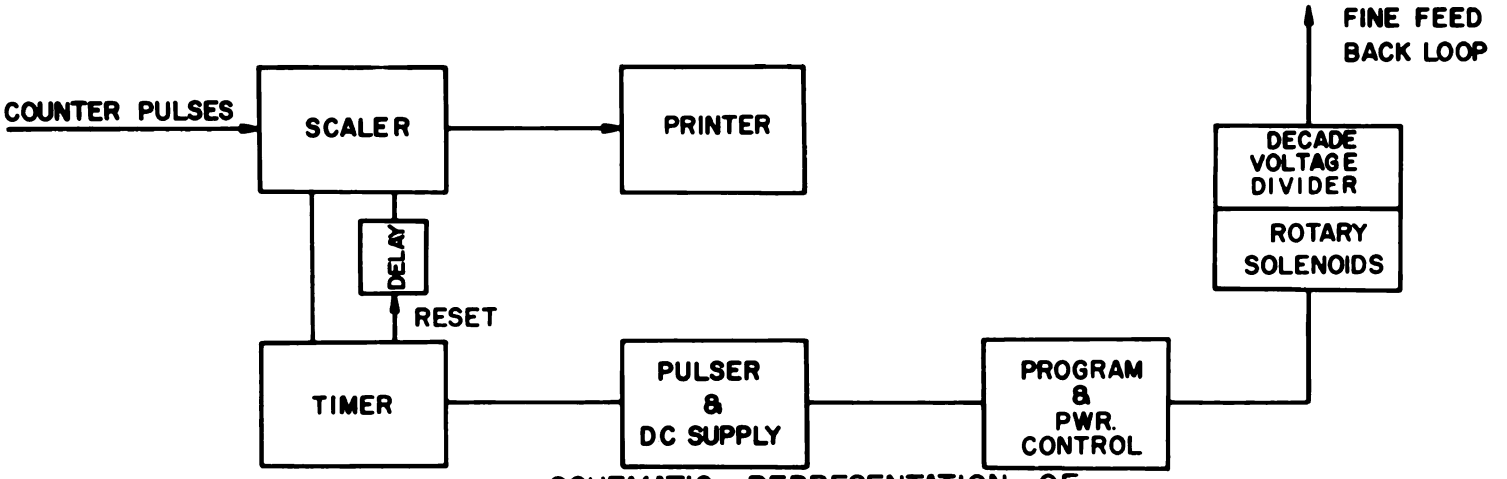

(1A) SCHEMATIC REPRESENTATION OF AUTOMATED DATA ACQUISITION SYSTEM

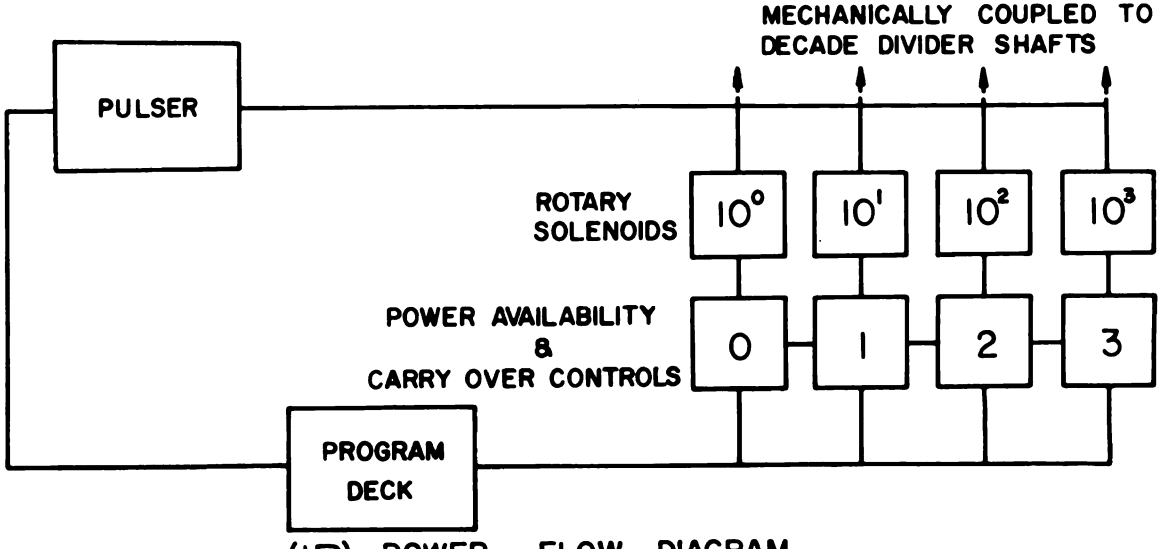

(1B) POWER FLOW DIAGRAM

FIGURE 1.

THE

With this the instrument is set for automatic operation and upon the elapse of the counting interval, the accumulated data will be printed out and the programmed momentum change will be made, after which another counting cycle will begin, and etc. This cycling operation will continue until the high side of the momentum region is reached, at which time the previous switches* may be thrown manually to their initial positions, thus stopping the whole procedure.

A variable delay relay delays the reset signal from the timer to the scaler. This is done both to give the rotary solenoids enough time to make a new momentum setting, and also for the field to stabilize. For a typical operation, a four second delay is sufficient to satisfy the above requirements.

Figure 1B shows the power flow to the individual solenoids and the elements that are responsible for the selective operation of each solenoid. Information is stored by means of the program deck, also shown in fig. 2, which tells a solenoid (R.S.) how many steps to advance. All four solenoids may mutually use this information at any given time. The notation 10^0, 10^1, 10^2, 10^3, refers to the divider decades (singles, tens, hundreds, thousands, respectively) that are coupled to

---

*Only S_4 and the scaler count switch need to be returned to their initial positions.

[redacted]

THES

the rotary solenoids. Elements 0, 1, 2, 3, provide two functions. They give the stored information a direction of flow, namely by controlling the power availability they tell each solenoid when to accept or ignore the available information. They also perform the function of carrying over a solenoid to its starting or zero position. The connections of the top wafer of column 10^1, fig. 2, show how the rotary solenoid would be carried over from the eight to the zeroeth position,* e.g., 023480 to 023500.

Universal joint type couplings are used to connect the output shaft of the rotary solenoid with the decade divider momentum selection shaft. The mechanical alignment of these two shafts is critical.

Figure 2 shows the details of fig. 1B. Besides showing the permanent power connections it shows the program for a $\Delta = 20$ operation, i.e., decade divider will be stepped up in steps of 20 decade units. At the time that the print command is given the relay in the upper left hand corner is de-energized for a fraction of a second, providing the first power pulse to the loads that are ready to accept it, and initiating also the

---

*The positions that the rotary solenoid can assume correspond exactly to the wafer contact numbers as shown by refering to the top wafer of column 10^0. Decade divider positions 10 and 11 are vacant positions.

Figure 2. Details of Figure 1 (B) and $\Delta = 20$ Program.

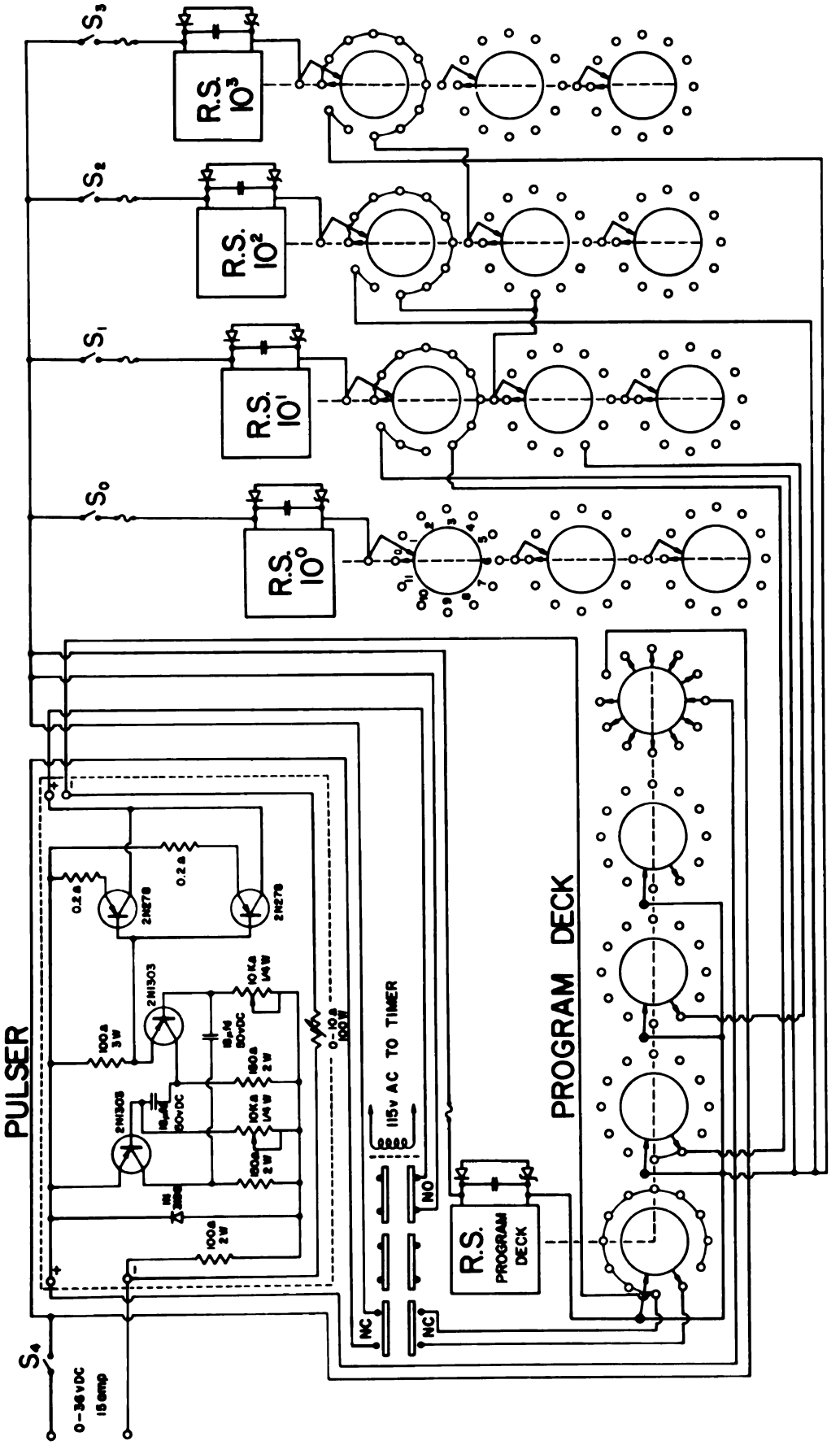

DETAILS OF FIG. 1B AND Δ = 20 PROGRAM

FIGURE 2.

operation of the pulser. The pulser will then provide eleven pulses and be turned off (by the last wafer in the program deck) bringing the wafer rotor tabs of the program deck to the initial position.* The pulser will remain off until the next print command is given. In other words, during this process twelve pulses are generated and all of them (or some number less than twelve) may be directed to pulse any of the four driving solenoids. For example by connecting the 11 and 0 contacts on the second wafer from the left (program deck), the 10^1 solenoid is permitted to turn two steps (1/6 revolution). If it is desired that the 10^1 solenoid would take, say, six steps then contacts 11, 0, 1, 2, 3, 4, would need to be mutually connected. Thus, information is stored in this relatively crude way. The carry over operation for the $\Delta = 20$ case is accomplished by mutually connecting contacts 9, 10, 11, of the top wafer in the 10^1 column. During the last operation the lower wafer provides power transfer to the 10^2 column.

With the present system the decade divider may be programmed to go unidirectionally in steps of 5, 10, 20, 25, 50, 100, 200, 250, etc. which is sufficient for

---

*The rotary solenoid of the program deck completes one full revolution.

THES

the typical problems encountered so far.* More versatility could be provided by a better memory, and by installation of bidirectional solenoids. The programming from one mode of operation to another, which takes now about two minutes, could be eliminated by prewired circuits. A program may also be incorporated which would cycle a given momentum region. An extra wafer would need to be used in the 10^3 column.**

---

*The Δ = 5, 10, 25, etc. programs are not shown in this diagram, since very little mental exercise is needed to program them once the fundamental operations of the Δ = 20 mode are understood.

**The third row of wafers in fig. 2 are spares.

[redacted]

THESI

CHAPTER III

POSTFOCUSING ACCELERATION FOR A $\pi/2$ SPECTROMETER

A. General Design Considerations

Detection of low energy (<5 kev) electrons with constant efficiency or transmission is a frontier region in beta-ray spectroscopy. Physicists have employed, with various degrees of success, several methods of detection of focused beams as they emerge from the spectrometer.[15] For example, it has been found that a detector consisting of a scintillator and a photomultiplier tube removed via a light pipe from the spectrometer magnetic field and cooled to liquid nitrogen temperatures can be used effectively to detect electrons above roughly 20 kev; however, below these energies one is confronted with varying detection efficiencies. The efficiency of the scintillator and photomultiplier combination decreases with decreasing energy, and careful detection efficiency curves must be run to insure reliable intensity measurements.[16] Electron multipliers may be used, but here again the detection efficiency is by no means constant for electrons of different energies. Most commonly, gas filled counters are employed. They require a window to keep the counter gas from leaking into the spectrometer vacuum system, i.e., an electron absorbing slab of matter is introduced into the beam path, thus

requiring the experimenter to consider its transmission properties. If the window is a very thin film, (say collodion, ~30 ug/cm^2), then electrons down to approximately 10 kev may be detected with 100% transmission. However, if the spectrometer is adjusted to focus electrons of lower energy, then absorbtion corrections have to be made.[17] If the detection of even lower energies is desired, then one will find that for the above mentioned film the transmission of electrons will stop completely at about 2.5 kev (so-called cutoff energy) where the gas counter becomes effectively useless. Its usefulness may be extended by the use of even thinner films. However, there is a practical limit to this since films below 10 ug/cm^2 (~1.1 kev cutoff) tend to be difficult to produce, tend to be leaky and destroy their usefulness by creating poor vacuum, and thus introducing another type of unreliability in measuring relative intensities. For example, an electron of 2.6 kev energy will have a probability of 0.03 to be scattered out of the beam while traveling through one meter in a vacuum of 10^{-4} Torr.[18] The author has found that it is possible by means of a support to manufacture windows $\gtrsim$10 ug/cm^2 which can maintain a vacuum better than 10^{-5} Torr and which will support counter pressures of 55 mm Hg for several weeks. The support that is used is an etched copper grid with approximately 55% transmission (Buckbee Mears Co.). The problem is far from solved, however,

since such windows will transmit electrons with constant efficiency only down to 5-6 kev in energy, and anything below that figure must be corrected for absorbtion. Thus the problem reduces itself to making another experiment, namely, the measurement of the absorbtion properties of the thin film, or using theoretical results which are questionable and certainly unreliable for precision spectroscopy.[19] This problem can be circumvented by the use of an electrostatic accelerating potential, e.g., between the detector and the spectrometer wall. By increasing the energy of the electron beam in this way, one can drive electrons through the window without absorbtion losses, (i.e., push the effective cutoff energy to negative values). It is possible in principle to detect with constant efficiency electrons approaching zero energy.

During the last fifteen years several investigators have attempted electrostatic acceleration.[15, 18, 20-29] Both preacceleration and postacceleration have been tried. The success has been only partial. Acceleration of the electrons at the source can lead very easily to defocusing problems unless extreme care is taken. This is especially true for precision instruments running at high resolution. Acceleration at the source also leads to a loss of effective resolution. Note that two lines separated by ΔE at E_1 now differ by ΔE at $E_2 = E_1 + E_{acc.}$ with application of a preaccelerating potential

TH

V ($E_{acc.}$ = eV). Noteworthy is that the electronics generating the preaccelerating potential must be very well regulated, e.g., better than 1:10^5 for an instrument such as ours. In these respects acceleration between the spectrometer exit port and the counter seemed to show more promise. However, previous attempts with postacceleration have lead to very serious noise problems whenever the accelerating potential brought up the electrons to the window cutoff energy. Giroux and Geoffrion[25] (fig. 3) have shown the sort of behaviour that was encountered. If the experimenter stayed below this potential, the method was partially fruitful, since electrons below the window cutoff were registered, although with variable transmission for different energies. Furthermore, it was possible to obtain a partial transmission curve for the window. The noise was identified as coming from outside of the counter window and it was hypothesized that it was due to secondary electrons, and/or ultraviolet radiation produced in the preliminary stages of discharge. The earlier investigators tended to use relatively high (~20 kev) accelerating potentials and heavy windows (~0.1 mg/cm^2). Work done by Achor[26] using potentials below 5 kev and films <10 ug/cm^2 indicated that spurious counts were not due to electrical discharges, but probably were due to essentially zero energy electrons being accelerated through the window.

With the above considerations in mind, we

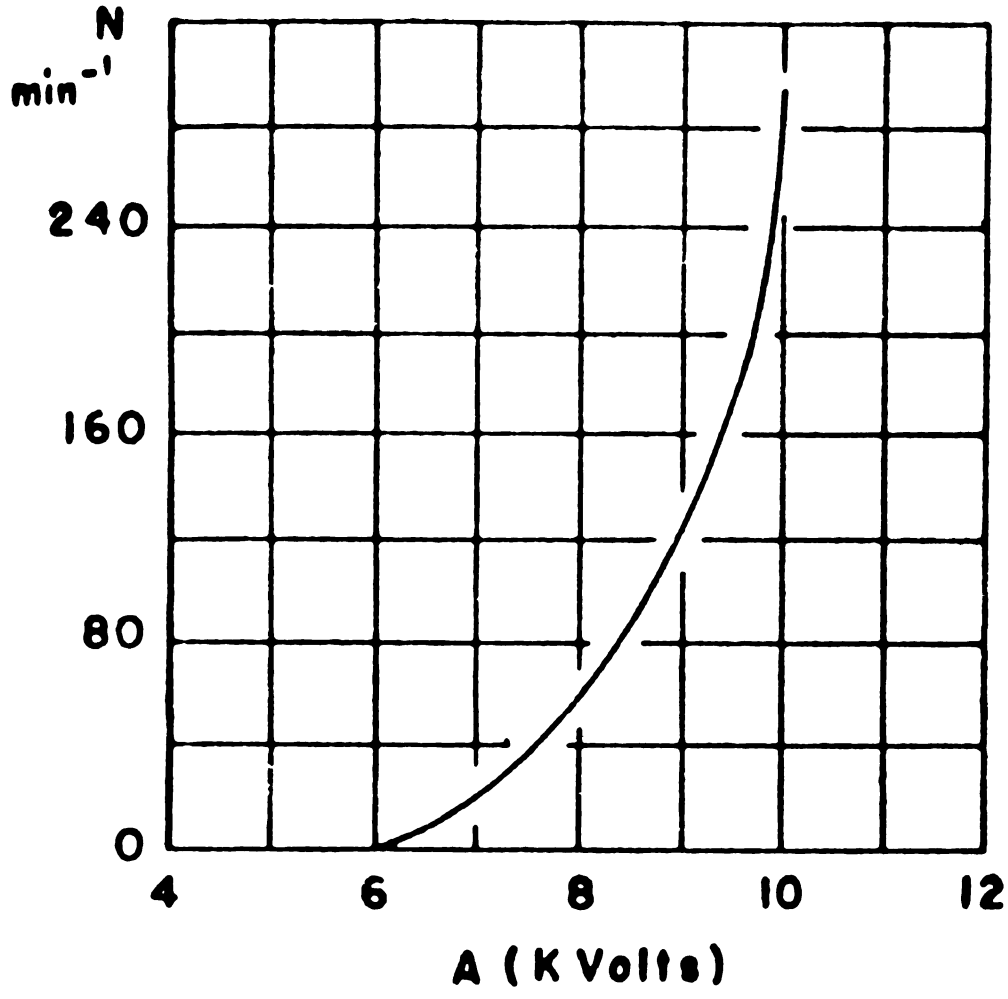

FIG. 4. Background count N (per min.) with the acceleration (A).

Figure 3. Noise vs. Post Acceleration Voltage from Giroux and Geoffrion, ref. 25.

decided that the most promising and the most practical approach would be to stay below 10 kev in voltage, and thus (possibly) avoid electrical discharges. This also simplified things in the sense that fancy high voltage electronics would not be necessary. The $\pi/\sqrt{2}$ spectrometer lends itself more readily to the use of a postacceleration technique than, say, a lens spectrometer, since a typical beam focus angle is about 5^{o}, and danger of spectral distortion due to the action of the accelerator electric field on the divergent beam can be kept at a minimum.

During the initial phases of the accelerator construction it was learned that Geiger et al[30] had used a simple version of an accelerator with the Chalk River $\pi/\sqrt{2}$ spectrometer with a 2.4 kev acceleration to study the M and N conversion lines ($\sim$3 kev) of Sm^{151}. This encouraged our decision to confine ourselves to lower accelerating voltages.

It was also learned that Mehlhorn and Albridge[31] were using a negative retardation potential to experiment with noise reduction. They have published a version of the technique used.[32] A retardation provision was therefore incorporated in our accelerator.

Other factors worth mentioning that were considered during the initial stages of construction and design were: (1) elimination of all steep electric field gradients and regions of high field in general; (2) mini-

THES

mization of high field in the immediate vicinity of the counter window where leaks were expected; (3) use of very regular and smooth surfaces; (4) cleanliness of the surfaces in the acceleration space; and (5) penetration of the electric field bubble from the accelerator field past the resolution defining slit.

B. The Acceleration Cell and Supporting Electronics

Figure 4 shows the combination of slit sizes and geometry which was used to run the L-Auger spectrum of In^{113m} (~2 to 4 kev). The spectrometer baffles were set so that the incident beam had a $\sim 5^{\circ}$ spread at the focus. The left side of the cell was tightened more firmly than the right to correct for approximately 1 mm deviation of the curving beam at point no. 3. A network of plastic screws was used to sandwich the plates together. Following is a point by point consideration of the various elements of the cell as they are shown in fig. 4.

(1,2) Counter Anode And Outside Wall

The basic counter design is described in Parker's thesis.[33] The anode is a 0.002" stainless steel wire, which is raised to the operating potential by a high voltage power supply stacked on top of the accelerator power supply by means of an isolation transformer. The counter is run in the Geiger-Muller region using a 67% argon- 33% ethylene mixture at 55 mm Hg with a resultant 12% slope. Teflon tubing is used to isolate the counter from the gas tank. The high voltage connections are made

THES

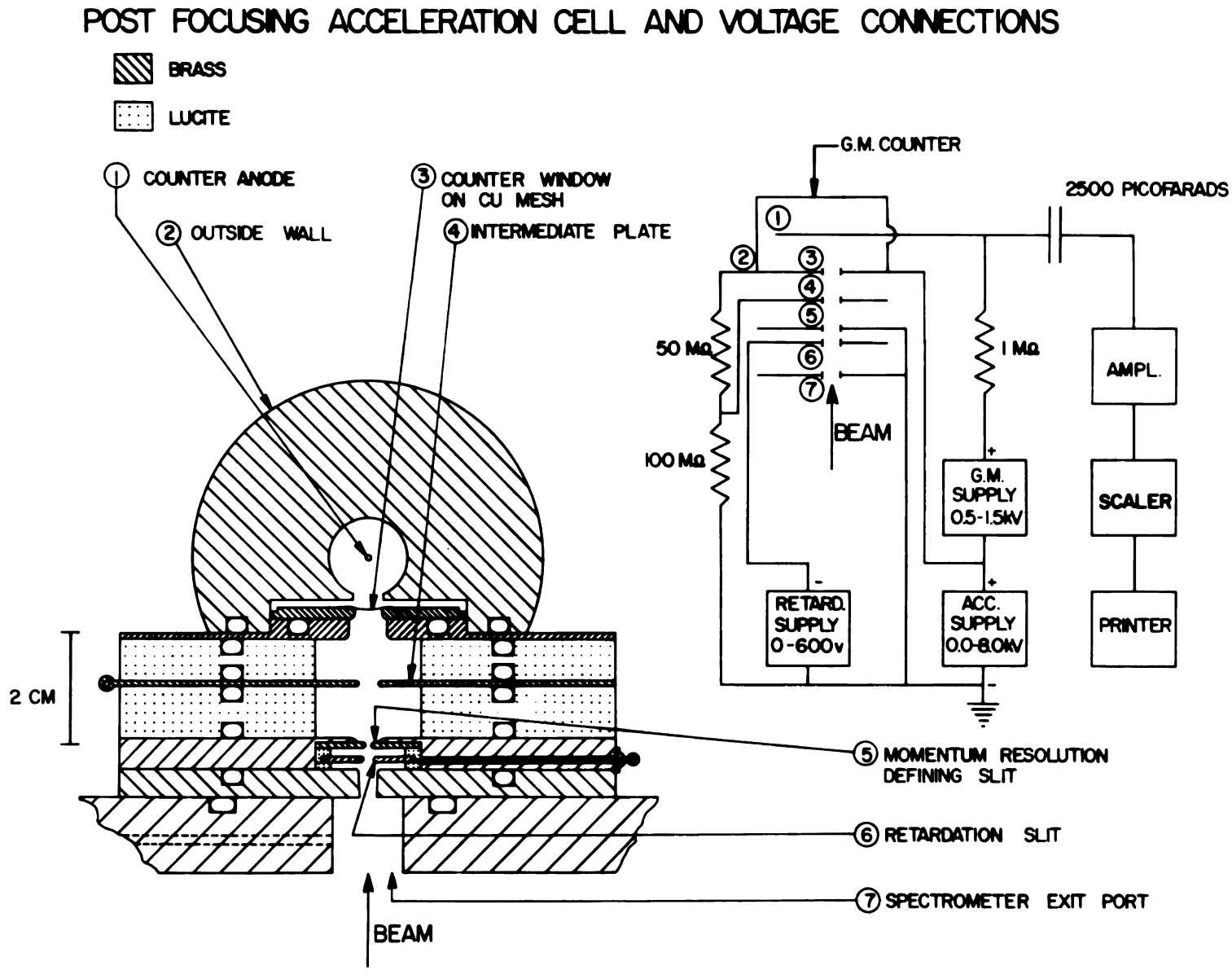

Figure 4. Postfocusing Acceleration Cell and Voltage Connections.

via a coaxial cable,* where the shield carries the accelerating potential and the inside conductor the counter potential. The counter wall and the window support are at a positive potential with respect to the spectrometer vacuum tank which is at ground potential.

(3) Counter Window on Copper Mesh

The windows are collodion, produced by the usual technique of dropping a solution of collodion in n-amyl acetate on distilled water. They are then mounted on the window plate and copper mesh support, which has been attached to the plate using low melting point solder paste** to minimize oxidation of the copper mesh. It is worthy to note that the window plate which supports the mesh and subsequently the organic film is highly polished on both sides, so that molecular attraction between the film and the plate together with the counter pressure pressing the film against the plate seems to give a relatively leak proof window seal. It was found that films of >10 ug/cm^2 will yield system pressures of 10^{-5} Torr or better when mounted in this manner.

(4) Intermediate Plate

The intermediate plate was introduced after experimenting with single insulating slabs of several thicknesses, and after an informal study of the relation-

---

*Belden 8239

**Force; American Solder and Flux Co., Phila.

THE

ship of system vacuum* to noise as observed with an oscilloscope. It was observed early in these investigations that by using accelerating potentials of greater than 3 kv, with a single insulator spacer of approximately 1 cm thickness, and with system vacuum~10^{-5} Torr, one induced the appearance of a new class of pulses (as distinct from the unmistakably identifiable counter pulses). Their amplitude and frequency seemed to increase with vacuum deterioration, and with the narrowing of the insulating slab (i.e., use of stronger electric field); or, the increase of accelerating potential. The number of true counter pulses started to increase only when the accelerating potential reached the cutoff energy of the window. It was possible to isolate the former rather dramatically by simply turning off the counter potential. The counter pulses disappeared while the others stayed. Unfortunately during these tests it was difficult to keep the variables under a strict quanti-

---

*"System vacuum" is used here synonymously with the extent of leakage of counter gas into the spectrometer main vacuum. The vacuum gauge was located in a draft free spot closer to the source than to the counter and therefore a vacuum check meant always that the vacuum as monitored in this spot was by a factor of one or two better than in the vicinity of the window.

tative control and therefore the author wishes to issue warning concerning the strength of the above statements.

It was felt that these residual pulses may have had origin in the accelerating volume, and possibly were due to the formation of positive ions which when accelerated to the cathode produced secondary electrons, thus producing a kind of capacitive discharge which could have easily reflected itself through the electronics into the counting circuit. The pulses were observed at the scaler input.

Another possible explanation hypothesized was that these curious pulses were due to some sort of surface discharge along the lucite wall, which was both dependent on the density of molecules near its surface and the strength of the electric field.

It must be remarked that these pulses at moderate accelerating potentials and good vacuum were smaller in amplitude than the counter pulses and could be rejected by raising the scaler treshold. It became impossible to do this, however, once ~ 4 kv were applied. It was decided then that an attempt should be made to see if any improvement occurs if most of the imparted energy is given immediately after the momentum resolution slit, allowing the region where the escaping gas concentration would be strongest to be a region of weaker field comparable in magnitude to what was considered to be a safe value from previous experiments. A happy medium

was attempted by slightly narrowing the original spacer and introducing an even narrower second spacer nearest the window, both being separated by an intermediate plate which would be set electrically at 2/3 of the total applied accelerating voltage. Of course, dimensional provisions had to be made to make sure that the beam could travel unhampered to the window. The spectrometer magnetic field was off during all above tests.

(5) Momentum Resolution Defining Slit

The momentum resolution defining slit (1 mm) consists of two pieces fit snugly into the cavity.

(6) Retardation Slit

The retardation slit (1.5 mm) consists of two similar pieces. The roles of the two slits may be easily interchanged, and it would be interesting to see the effect this has on the accelerator performance. The penetration of the electric field bubble into the region where the retardation slit is located is estimated to be about 10 volts with 8.0 kv acceleration. The advantage of its present location is that otherwise it would be moved into a deeper part of the accelerator potential and therefore would probably require more retardation voltage. The primary disadvantage to its present location is that it offers the incident beam, which misses the aperture, a negatively charged obstacle. This likely produces secondary electrons which are attracted in by the accelerating field and contribute to some of the noise

which will be discussed in the following section.

(7) Spectrometer Exit Port

The spectrometer exit port is actually preceded by a vacuum gate which is not shown.

The basic material used for the electrodes is yellow brass (67% Cu-33% Zn). The counter material is also brass with a somewhat higher content of zinc. The electrode surfaces were polished thoroughly starting with rough sandpaper and finishing with emery polishing paper, and effort was expended to manufacture a special rounding tool for rounding the internal edges (0.12 cm). Before assembly and attachment to the spectrometer the surfaces were further cleaned with Brasso and washed with benzene. Great caution was of course taken to avoid introduction of foreign materials on the electrodes.

Home made r.f. oscillator type high voltage supplies are used, with some special circuitry for the counter supply. Maximum current output is about 25 uamp each.

C. Operation and Performance

After the accelerator was assembled as depicted in fig. 4 it was observed that with no acceleration and retardation fields the accelerator hardware had introduced no changes in the beam transmission or instrumental resolution, as a matter of fact there appeared a slight improvement in the intensity of the Auger K-L_2L_3 line (20.1 kev), which was used in making this transmission

THES

test. Actually in the preliminary studies a 0.5 mm momentum resolution defining slit was used.* The author considers that the primary weakness of the accelerator in the above form is the danger of production of secondary electrons due to the large number of slits and edges along the beam path. However, the transmission study seemed to indicate that this fear is probably unwarranted.

We also observed that when the accelerating field was applied (no retardation), the earlier discussed non counter pulses appeared only after reaching ~6 kv accelerating voltage and were small enough at 8 kv (maximum range of supply) so that they could be rejected by changing the scaler treshold. The ratio in amplitude of counter to noncounter pulses was about 5:1 for 10^{-5} Torr. The ratio of their durations was approximately 3:5. The number of counter pulses increased with accelerating voltage (refer to fig. 5), regardless of whether or not a source was present, although the plateau level for the case of the source was higher. It could be raised even further if the ionization gauge degas current was turned on. Fortunately the application of the retardation

---

*The change of the width of the momentum resolution defining slit from 0.5 mm to 1.0 mm had no effect on the accelerator performance. The plateau level of the type shown by the top curve of fig. 5 increased in going to the wider slit.

THE

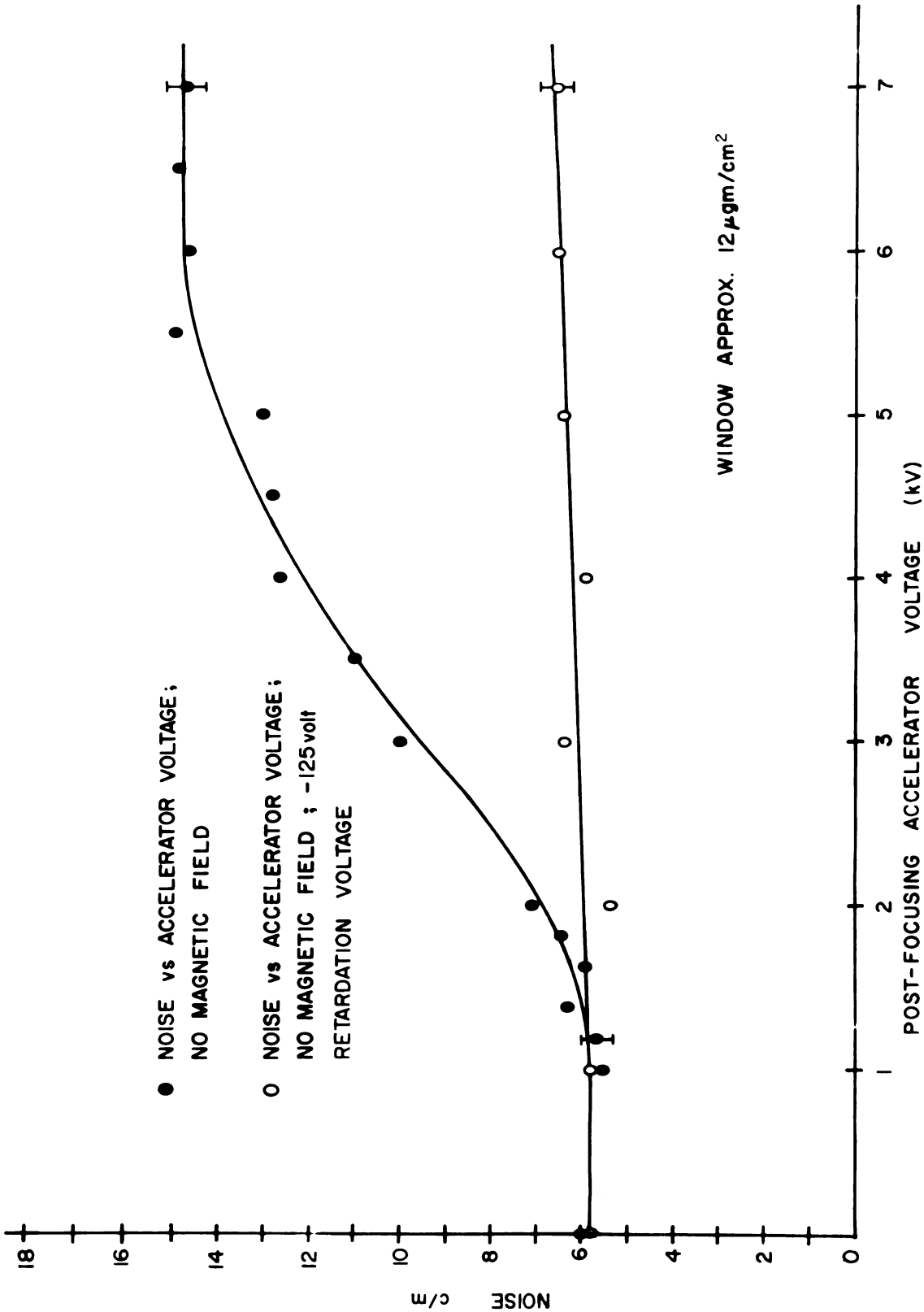

Figure 5. Noise Curves Showing Retardation Effect.

[redacted]

41

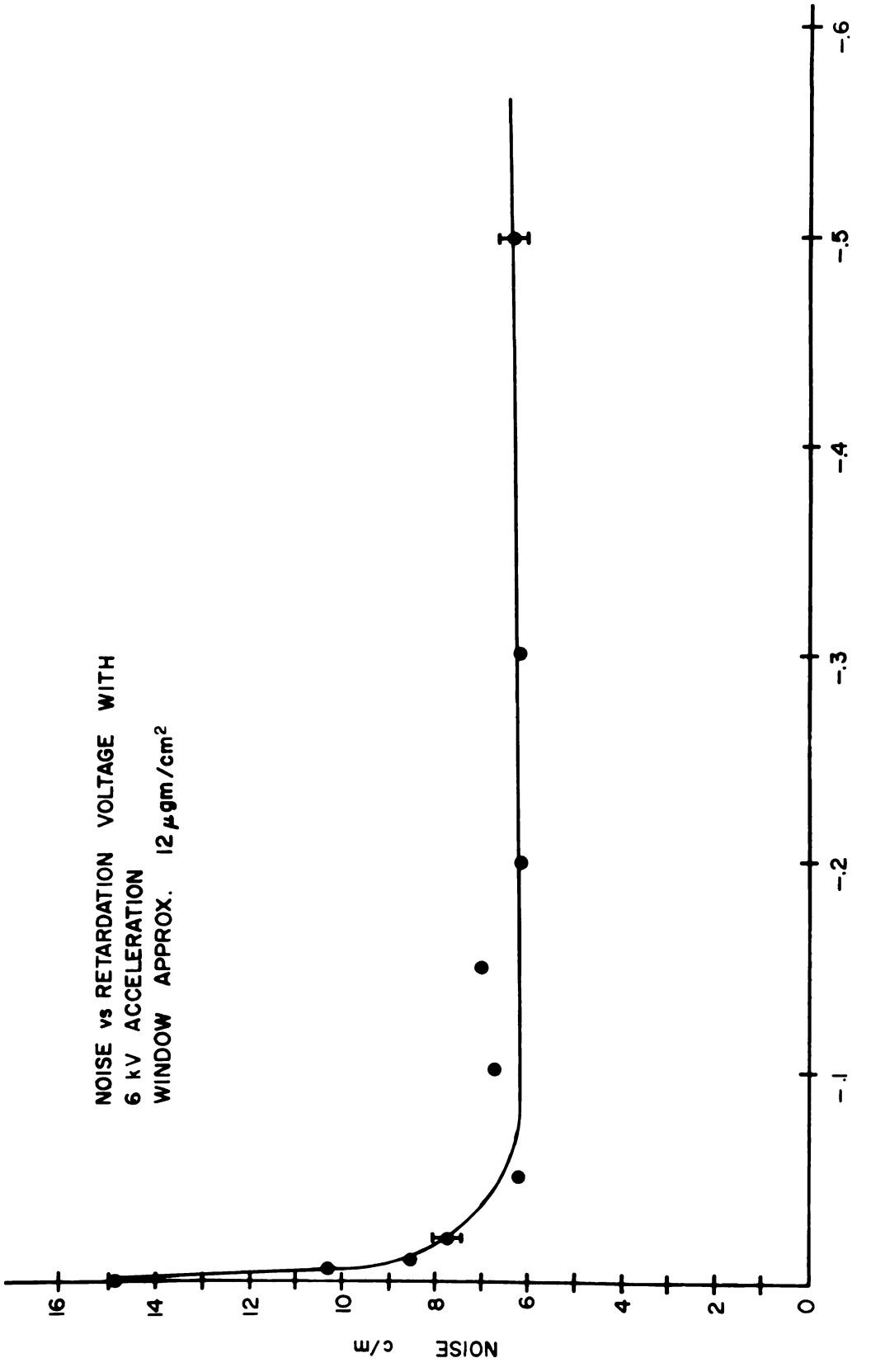

Figure 6. Noise vs. Retardation Voltage with Fixed Accelerating Potential.

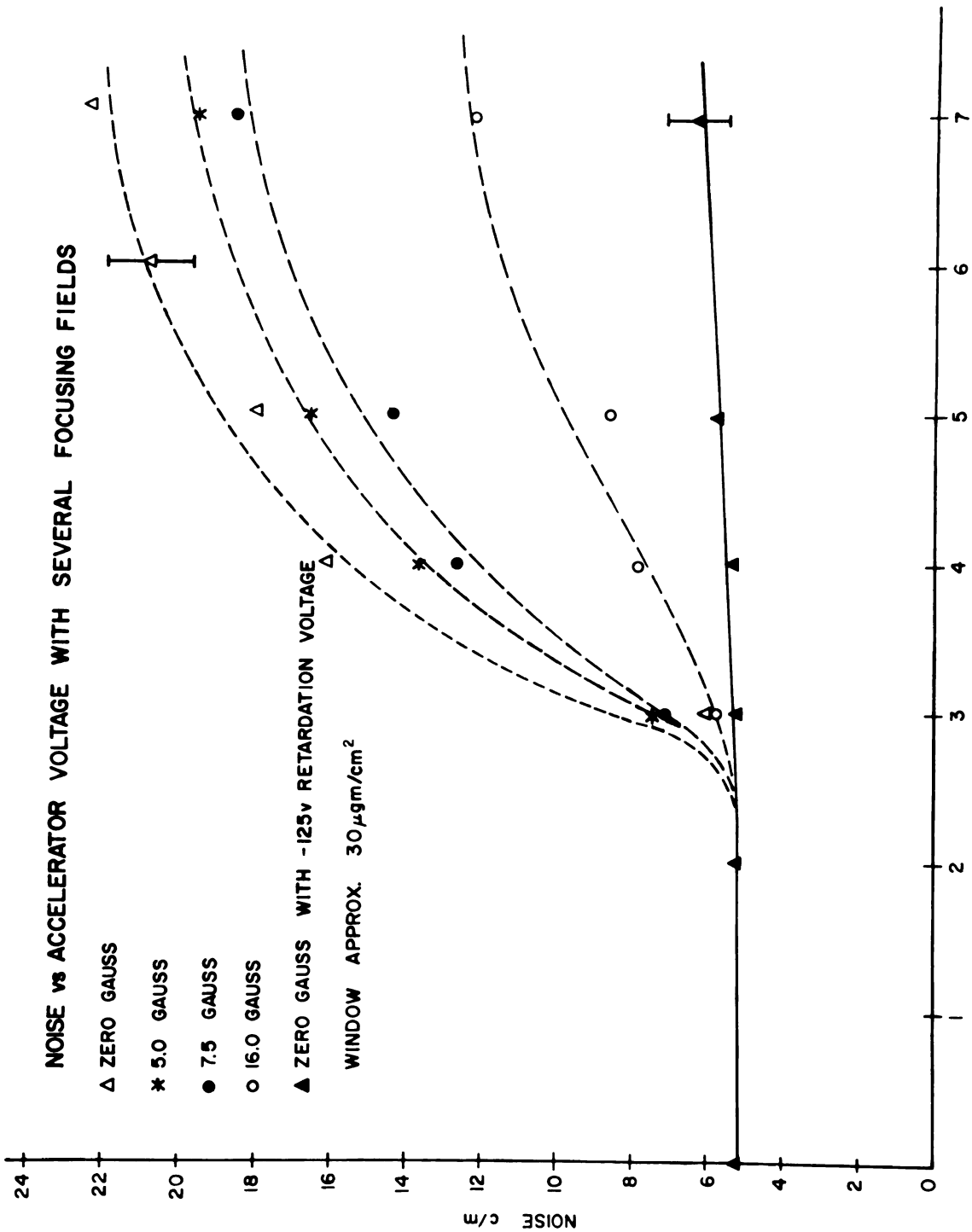

Figure 7. Noise vs Accelerator Voltage with Several Focusing Fields.

potential, fig. 6, (no spectrometer magnetic field) was able to reduce this noise to nearly natural background. The lower curve in fig. 5 shows the retardation effect along the full accelerator range.* With this information on hand, one is tempted to say that indeed the top curve in fig. 5 represents the delivery of low energy electrons from the main vacuum system to the detector. This is, of course, most strongly substantiated by the fact that they may be repelled by the application of the retarding potential; and by the results shown in fig. 7. These results show the noise dependence on the spectrometer magnetic field (no source), suggesting the possibility that some of the electrons which have been attracted by the accelerating field from the main vacuum tank are being removed from detection by the action of the magnetic field.

Further, it is interesting to note that the departure point of the retarded and the unretarded curves (say, fig. 5) corresponds very closely to the cutoff energy of the window. This point of departure of the two curves was, for all windows tried, consistent with the cutoff point computed from the estimated window thicknesses.[17] Noteworthy also is the fact that for the $\sim$12 ug/cm^2 window the shape of the curve corresponds

---

*The accelerator supply delivered only 7 kv maximum at the time these curves were run.

very closely to the absorbtion curves by Lane and Zaffarano.[17] However, since fig. 6 says that the energy of these low energy electrons floating in the spectrometer tank ranges, say, from 0 to 130 ev, then the departure point of fig. 5 is somewhat cloudy. For that reason and the fact that Lane and Zaffarano give very uncertain figures for their film thicknesses, a strict comparison between Lane and Zaffarano curves and the curve of fig. 5 is not made. The difference between the lower curve in fig. 5 and natural background is probably due to events in the acceleration space itself.

Considerable time was spent studying the effects of the post acceleration cell once the spectrometer was allowed to focus an electron beam. It was found that at about 20 kev, as mentioned previously, there seems to be no defocusing, fig. 8. However, there was a noise contribution to the line which was roughly dependent on the beam strength, e.g., $\lesssim 2\%$ at 6 kv acceleration, and decreased as the accelerating potential was lowered. This appears to be far superior to anything previously reported.[32] At lower energies there was no simple way to check the accelerator performance without a strong isolated line in the region of interest. By running curves of the type shown in fig. 8 (left) it was possible to show, however, that defocusing is negligible for this resolution. This was done by a point by point comparison of neighboring shapes both for the case of acceleration

and no acceleration. Examination of peak to valley ratio of both curves (using a rough absorbtion correction) yielded a accelerator introduced noise figure of about 1% of beam strength for this energy region. The insert shows graphically the growth of the L_3-M_4M_5 peak with accelerator voltage. No inconsistancies were found within statistics. Further, the insert demonstrated (although this is not indicated on the graph) that the introduction of 7 kv accelerating voltage did not shift the line position, thus encouraging the belief that no serious artificial energy shifts were introduced in the L-Auger spectrum (~2 to 4 kev). An extrapolation of the good results of performance in this energy region therefore seems appropriate down to at least 1 kev.

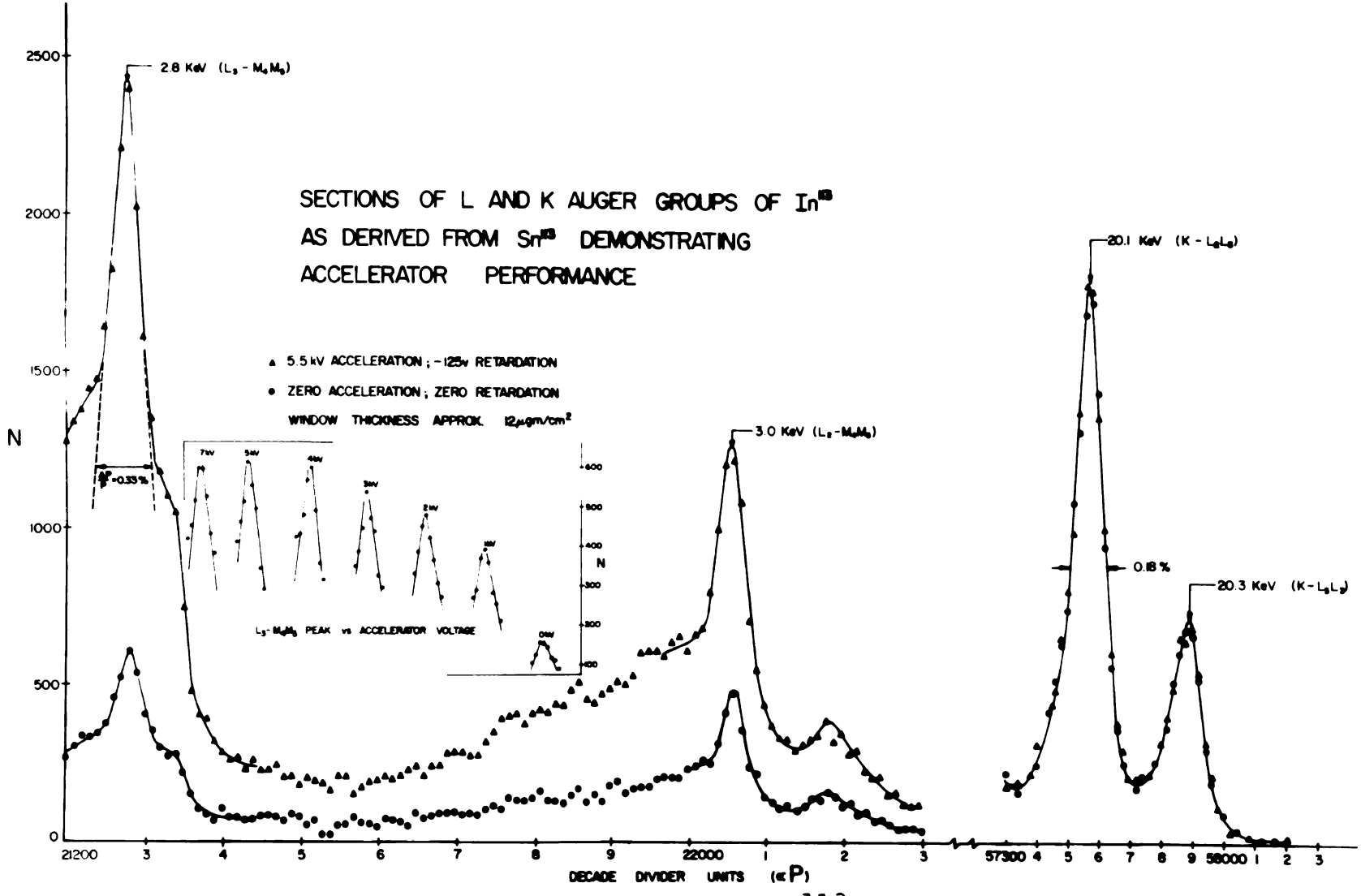

Figure 8. Sections of L and K-Auger Groups of In^{113} Demonstrating Accelerator Performance.

CHAPTER IV

THE L-AUGER SPECTRUM OF IN^{113} AS DERIVED FROM THE ELECTRON CAPTURE DECAY OF SN^{113}

A. Introductory Remarks

Chapter III represents the most serious expermental problem that needed to be solved, namely, the extension of the low energy range of the spectrometer by means of postfocusing acceleration.

Another important problem was the production of a very thin source in order to reduce the number of energy degraded electrons due to self-absorbtion by the source. Source absorbtion effects can be serious at the energies that were studied since they introduce long tails to the low energy side of monoenergetic electron lines and increase their width. This effect tends to defeat the high resolution capability of the spectrometer and also serves as a handicap in the analysis of the spectrum. A later section of the chapter is devoted to the description of the source production technique that was required to minimize this effect.

The reasons for the choice of the electron capture decay of Sn^{113} as the subject of study were stated in CH I and are given again here for completeness.

First, the L-Auger spectrum of a medium Z atom

had never been studied previously. This was a matter of interest by itself.

Second, Z = 49 is a good place to look for double vacancy effects following K-LL transitions since the K-Auger yield, a_K, is a factor of three greater for this Z (ref. 1) than for, say, Z = 80.* The energies of L-Auger spectra decrease with decreasing Z enhancing the experimental difficulties. Z = 49 was thought to be a good compromise of fairly high Auger yield and yet high enough L-Auger energy.

Third, Sn^{113} was easy to produce due to a large neutron capture crossection,[12] and could be easily separated from Sn^{112} by an electromagnetic mass separator.

Fourth, previous experience in this laboratory of separating trace amounts of In^{113} from Sn^{113}, using volatility differences of the two elements to an advantage, gave us the capability of observing the Auger contribution due to the conversion process alone. Figure 9

---

*a_K is the probability that a K vacancy will be filled by means of an Auger transition. The L Auger yields, a_{L_1}, a_{L_2}, a_{L_3}, (similarly defined) are also substantially higher for this Z, meaning that the L-Auger spectrum intensity would be similarly higher for the same number of radioactive atoms than for a heavy element (with other factors assumed to be constant).

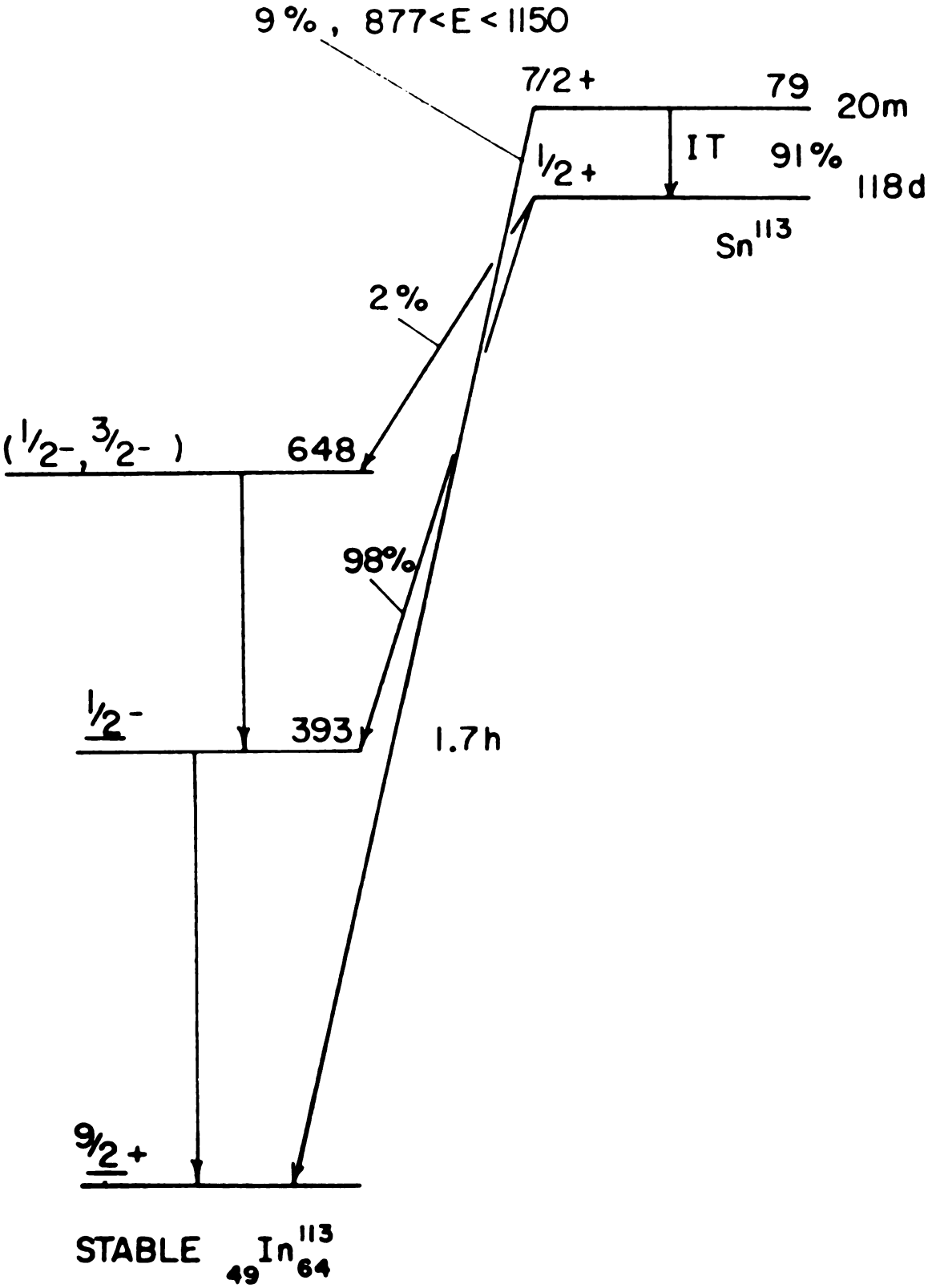

Figure 9. Decay Scheme of Sn-113 from Schmorak, Emery, and Scharff-Goldhaber, ref. 12.

shows the decay scheme due to Schmorak, et al.[12]

The strong features of the decay, such as the capture branch leading to the 393 kev isomeric state of In^{113m}, have been well established and have been recently reaffirmed by a number of investigators.[12, 34-39]

The measurements of the orbital capture ratio L/K and the decay energy to the 648 kev state[34, 39] and the 393 kev state[40, 41, 42, 43] have been inconsistent, however, providing ample motivation for further study and reinterpretation of existant data.*

Since the focus of the present investigation is on the measurement and interpretation of the L-Auger spectrum, the author will confine himself to a discussion of the Auger effect. Any detailed discussion of the orbital electron capture process will have to be postponed until the complete electron spectra of the Sn^{113}-In^{113} system are run and interpreted.**

---

*E.g., G. Manduchi, et al[40] report L/K = 0.44 for the capture branch leading to the 393 kev state. This is hard to reconcile with the results of other investigators.

**The K-LL group has just been run. The K-LX, K-XY groups and the conversion electron spectra will be measured in the near future. Preparation is being made for the study of the Auger spectra due to the conversion process alone.

B. The Auger Effect

The Auger effect has been recently described in two review articles by Listengarten[44] and Sant'ana Dionisio,[45] and is discussed in some detail by Burhop.[46] The recent edition of Kai Siegbahn's α-β-γ-Ray Spectroscopy[1] also has a section on the Auger effect, as described by Bergstrom and Nordling. Its discovery was made by Pierre Auger[47] in 1925 who hypothesized that electron tracks which were found in photographic emulsions, irradiated by x-rays, were due to nonradiative atomic transitions where a bound atomic electron is ejected into the continuum as an alternative deexcitation mode to x-ray emmission.* In other words, an inner vacancy is filled by an outer electron and instead of creation of a photon, the excess energy is carried away by another bound electron. It may be described best by writing the transition probability, λ,

$$\lambda = \text{CONST.} \left| \langle \psi_x \varphi_\ell | \mathcal{H}_{i\ell} | \psi_i \varphi_i \rangle \right|^2$$

---

*The Auger process has also been observed in mesonic atoms[48] where a π or a μ meson fills a primary vacancy.

where,

ψ_i, ϕ_i = initial bound state wave functions, representing the two electrons that will participate in the Auger transition.

ψ_f, ϕ_f = final state wave functions where one is a bound state and the other is in the continuum.

$\mathcal{H}_{i,f}$ = electrostatic interaction.

The usual notation that is used to denote Auger lines is based on a j-j coupling scheme and, thus, as an example, we might have a K-L_1L_3 transition which in terms of the above notation would be represented as follows:*

$$\lambda = \text{CONST.} \left| \langle 1s_{1/2}\, \underline{k} | \mathcal{H}_{i,f} | 2s_{1/2}\, 2p_{3/2} \rangle \right|^2$$

where, K = $1s_{1/2}$, the primary vacancy.

L_1 = $2s_{1/2}$, the electron that fills the vacancy.

L_3 = $2p_{3/2}$, the electron to be ejected.

$\underline{k}$ = the ejected electron.

---

*Electron indistinquishability and consequent need to consider both direct and exchange transitions is neglected for demonstration purposes.

In practice when the primary ionization may occur in any of the subshells, it is possible to have the following groups of Auger electrons: K-LL, K-LX, K-XY (X, Y represent shells with principal quantum numbers (n) greater than two), L-MM, L-MX, L-XY, and M-XY, etc. (M stands for n = 3).

A separate low energy group of the type L-LX is also possible. These are called Coster-Kronig transitions.[49] Recent theoretical investigations of the Coster-Kronig type of transitions have been made by Asaad[50] and Callan.[51]

The K-Auger groups have been studied theoretically, with the main emphasis on the K-LL group.[52-57] There is very little theoretical data for the L-Auger groups. The work of R. A. Rubenstein[58] is the only known theoretical calculation for medium Z element, Z = 47. The treatment uses pure Russel-Saunders coupling as an approximation.

The experimental studies of the L-Auger spectra have not been numerous, primarily because of the great experimental difficulties. Only with recent improvements of beta ray spectrometers and source production techniques have these measurements been attempted. The measurements that have been made are all for the heavy elements[59-66] where the spectra low energy endpoint is high enough so that no special electron detection techniques are necessary.

C. Source Preparation

Isotopically enriched (~72%) Sn^{112} in oxide form was irradiated in the Oak Ridge Research Reactor for seven weeks. The irradiated material was converted by ORNL to metal powder by heating. Because the specific activity of the above substance was far too low in order to produce a thin source for studying low energy spectra, the isotopic mass separator of the Argonne National Laboratory was subsequently used to reduce the stable Sn^{112} and other impurities.

Preparation of sources for beta-ray spectroscopy by means of electromagnetic mass separators has been excellently reviewed by I. Bergstrom, et al.[67] One of the key problems is that with typical separator accelerating voltages, which usually are about 40 kv (for optimum separation efficiencies), the ion beam will penetrate into the target material deeply enough such that when the source is studied by means of a high resolution spectrometer one finds serious tailing effects of monoenergetic electron lines. This is due to the fact that the electrons in leaving the target (which is now the source backing material for the spectrometer study) suffer energy losses. This effect is already serious for, say, ~20 kev electrons when the ion beam is deposited at 40 kv onto an Al target. Since the L-Auger spectrum is in the range of ~2-4 kev, the above effect was expected to be even more serious. Therefore, a reduction in the

ion beam energy and minimization of penetration effects was absolutely necessary.

Therefore, the general scheme for the production of a high specific activity (thin) spectrometer source, using the mass separator, was one that involved a beam deceleration technique in order that the beam energy striking the target would approach zero. This had been tried before with various degrees of success.[67] In our case it turned out to be somewhat disappointing since the deceleration system produced very localized intensity distributions (1x1 mm^2) resulting (what we believe) in a "thick" source in the conventional sense.* The study of these sources by means of the spectrometer showed very serious energy losses and tails. Further, since vertical-longitudinal Al masks (1x18 mm^2) were interposed between the ion beam and the source backing (or the target), to better define the source distribution for the spectrometer, one would have expected a vertical-longitudinal distribution on the backing.** If anything, the deposit seemed to be perpendicular to the expected direction. Later it was discovered that the retardation system was

---

*The beam was gently laid down at an estimated energy of 0.5 to 1.0 kev for a dozen or so sources that were prepared.

**The unretarded beam is vertical and about 2x10 mm^2 in corssection.

indeed producing a horizontal distribution of source material. This was not obvious by looking at the localized source intensities on the targets because the masks had cut out some of the horizontal line. This effect was pinned down by running autoradiograms of the masks which showed quite clearly that the deposit was horizontal.* [68] After lengthy studies of above sources with our spectrometer (with post-acceleration) it was determined that they were inadequate for studying the L-Auger spectrum due to exibited thickness effects. A way had to be found to produce a usable source.

The source that was finally used for our L-Auger study was manufactured in the following way. The separated Sn^{113} beam was collected on a tantallum strip 2.000" by 0.155" by 0.005". It was then cut along the length into roughly 0.030" wide strips. These were connected one at a time to act as filaments in a vacuum evaporator set up. The evaporator vacuum was about 10^{-5} Torr. A 0.5x18.0 mm^2 Al mask was used to define the

---

*The question as to why this was happening is still an open one. There seems to be a striking resemblance to the optical aberration called coma, which is produced by light entering a lens from the point off the axis. The problem is still under study at Argonne.

source deposit upon a ~1.5 mg/cm^2 Al backing. The filament was flashed to very dull red to remove any very volatile foreign matter. Then the mask and backing were introduced and the filament was flashed twice to dull red. These steps were enough to remove most of the active material from the filament. The remaining activity was probably due to imbedded atoms since even at low deposition voltages, 0.5 to 1.0 kv, there is some penetration into the tantallum.[67] Two such filaments were used up to produce our source.

D. Measurement

The Michigan State University π/2 double focusing iron-free beta-ray spectrometer[10] was used for this study. It was adjusted for a momentum resolution of 0.12%. The 2 to 4 kev region of the L-Auger spectrum was scanned by taking 1000 points at equal decade divider intervals. The focused beam was post-accelerated by a 5.5 kv electrostatic potential as described in CH III. The voltage was increased to 6.5 kv when investigating the region down to 1.0 kev. The counter window was collodion (12-15 ugm/cm^2) supported in the same manner as discussed in CH III.

The relative precision of measurement of momentum was better than one part in 10^4.

The spectrometer vacuum was maintained at 5×10^{-6} Torr. There appeared to be a deterioration of source quality with time and over a period of 550 hrs the slope

and peak intensity of the most prominent L_3-M_4M_5 line (fig. 10) decreased by 23% and 13%, respectively. This is attributed to contamination of the source surface by vacuum pump oil. Some source loss may have also occured. It was estimated to be less than 3%, on the basis of observation of the K-L_2L_3 line. Checks of source quality, approximately 1600 hrs later, indicated that the deterioration was progressing at a decreasing rate and most of the damage had been done within the first 400 hrs or so. This did not affect the data significantly since several passes were made over the spectrum. Each pass over the regions of structure averaged about 60 hrs and during this time source quality changes could be considered insignificant.

The earth's magnetic field was compensated to $\leq$0.2 mgauss on the vertical component and 0.1 mgauss on the horizontal components by four daily checks with a saturable strip magnetometer.* Short term drifts of the vertical component of the earth magnetic field did not have serious effects on the net focusing field since the spectrometer is designed to compensate immediately for such changes.[10]

E. The Spectrum and Discussion

The spectrum is presented in figure 10 which also

---

*Magnaflux Corporation, Chicago, Illinois.

shows the energy ranges of the different L-Auger groups. The interpretation of such a spectrum is not an easy problem.

By way of illustration, let us consider an ideal set of conditions which would be desirable from the standpoint of an easy study and clear cut interpretation of the L-Auger structure. These conditions could be described as follows:

(1) Existance of no primary vacancies except in the L_3 shell.*

(2) Choice of atoms of large enough Z such that the two vacancies produced in the M shell during a L_3-MM Auger transition could be described by pure j-j coupling.

(3) Capability of manufacturing a high specific activity source of one or two atomic layers in debth, which would exibit no source thickness effects.

(4) Use of a conducting source backing, say $\sim$10 ug/cm^2, to avoid the classical problem of back-scattered electrons which produce an ambigous

---

*K. Risch[69] has demonstrated that it is possible to create vacancies in the L_3 subshell of bismuth by means of monochromatic x-rays without ionizing the L_1 and L_2 shells and in this way study the resulting isolated L_3-Auger spectrum.

background under the spectrum.

(5) Unlimited resolution.

Under these circumstances the L-Auger spectrum would consist of the L_3-XY groups (X = M,N; Y = M,N) due only to the L_3 vacancies (refer to fig. 10 for the L_3 energy ranges). The widths of the lines would be merely the sum of the widths of the atomic states involved in a given transition. The backscattering would probably be negligible. Any overlap of lines would be due only to the overlap of atomic widths.

If in the light of the above considerations we examine our spectrum, we find that:

(1) The primary vacancy contributions to the L subshells are due to, (a) orbital electron capture, (b) conversion process, (c) transfer of holes from the K shell by means of radiative transitions, and (d) transfer of holes from the K shell by means of Auger transitions (K-LL and K-LX). Table I gives a first order approximation of what would be expected for the relative vacancy distributions per disintegration for the three different L subshells. The 2% capture branch to the 648 kev state (fig. 9) has been neglected. Thus, we see that the set of primary vacancies which give our spectrum comes about in a complicated way and the spectrum (fig. 10) is now a superposition of the L_1-XY, L_2-XY, and

TABLE I. Estimated Relative Vacancy Distribution for the K, L_1, L_2, L_3 Shells

	Process Creating Vacancy	K	L_1	L_2	L_3
a	Electron Capture	0.871	0.1047	0.0022	____
b	Internal Conversion	0.282	0.0410	0.0061	0.0082
c	Radiative Transfer from K		____	0.2660	0.5240
d	Auger Transfer from K		0.0740	0.0915	0.1300
e	Sum	1.154	0.2197	0.3658	0.6622

(a) Calculated using Rose and Brysk formulas (ref. 6).

(b) Calculated using tables of internal conversion by Sliv and Band (ref. 1).

(c)(d) The K flourescence yeild was assumed $w_K = 0.83$ (ref. 1). The number of vacancies forming in each of the L subshells per vacancy filled in the K shell was taken from Listengarten (ref. 56).

L_3-XY groups with very serious overlaps starting at approximately 3130 ev (22500, fig. 10). Further, it is not possible to deduce what the relative intensities of the three major groups might be on the basis of the figures of row (e) Table I, because the partial Auger yields a_1, a_2, a_3 are not known. They are related to the Coster-Kronig yields, f_{ij}, and the partial fluorescence yields, w_i, (i,j = 1,2,3,) in the following manner,*

$$\omega_1 + a_1 + f_{12} + f_{13} = 1$$
$$\omega_2 + a_2 + f_{23} = 1$$
$$\omega_3 + a_3 = 1$$

and are known very imprecisely. This is also true for the fluorescence yields although these are known to be 2-3% for Z = 49.

The most important C-K transitions for this Z have been found to be of the type L_1-$L_3M_{4,5}$ (refs. 44 and 50). Their effect would be

---

*f_{ij} is defined as the probability that the i shell vacancy will be filled by a transition of the type L_i-L_jX,Y. a_i is defined as the probability that the i shell vacancy will be filled by an Auger transition of the type L_i-XY. w_i is defined as the probability that the i shell vacancy will be filled by an x-ray transition.

to create additional vacancies in the L_3 subshell (in addition to those set forth in Table I). Further, because they cause ionization of the $M_{4,5}$ shells, the subsequent L_3-$M_{4,4}M_{5,5}$ lines would be shifted due to the fact that the $M_{4,5}$ electrons that are to be ejected are now more tightly bound. This phenomenon has been observed in x-ray studies. Refer to references 70 and 71. In our case this will be neglected since by Table I the most intense L-Auger group is due to the L_3 vacancies and the L_1-$L_3M_{4,5}$ transition can be considered negligibly small in terms of intensity contribution, particularly, since the primary L_1 vacancy is by a factor of three less than the L_3 vacancy.

(2) For the case of Z = 49, pure j-j coupling is not a good approximation. Both theoretical deductions by Burhop and Asaad,[50, 52] as well as experimental measurements of the K-LL group, e.g., by R. L. Graham et al,[72] have shown that intermediate coupling features play a strong role for $Z \sim 50$. That is to say, in the interpretation of the spectrum we can no longer ignore the fact that a j-j coupled line may have associated intermediate coupling satellites. In previous studies of L-Auger spectra of high Z elements a discrete j-j coupling approximation

was still warranted.

(3) Source thickness effects as exibited by long tails are important handicaps in the analysis, particularly, since they vary over the spectrum becoming more severe towards lower energies. The possibility of discrete energy losses of electrons as they emerge from the source must also be considered. A characteristic bump on the low energy side of a line when particles must travel through a thick source has been observed by, e.g., Nordling, et al[73] and J. S. Geiger, et al.[30] It has been attributed to quantization of inelastic energy losses of the electron, and has been treated theoretically by Bohm and Pines.[74]

(4) Backscattered electrons are estimated to give a background contribution of 5-10% of intensity making it difficult to draw a base line for the spectrum.

(5) Even though the spectrometer resolution is excellent (0.12%) the above reasons make it impossible to isolate a "standard" line shape in a clear cut manner. Moreover, at this resolution and energy the natural widths of the lines play an important role. Due to the fact that no measured or calculated values of L widths for Z = 49 exist, they could not be

taken into account during a crude line fitting effort. As a guide in analysis extrapolated values were used for the L widths obtained from J. S. Geiger, et al,[30] and Listengarten.[44]

Clearly, the interpretation of this spectrum is a difficult problem. Table II gives the measured positions of lines together with the values calculated by means of the following expression, first suggested by Bergstrom and Hill,[75]

$$E(L\text{-}XY)_Z = E(L)_Z - E(X)_Z - E(Y)_Z - \Delta E_{XY}$$

where,

L = primary vacancy in any of the three subshells.

X,Y = resulting vacancies in any of the succeeding subshells of major shells.

E(L),E(X),E(Y)= binding energies of the respective subshells.*

$$\Delta E_{XY} = \Delta Z(E_{Z+1}(Y) - E_Z(Y))$$

where, ΔZ was allowed to take values 0.55; 0.67 for tran-

---

*Binding energies used were obtained from tables in reference 1 due to S. Hagstrom et al.

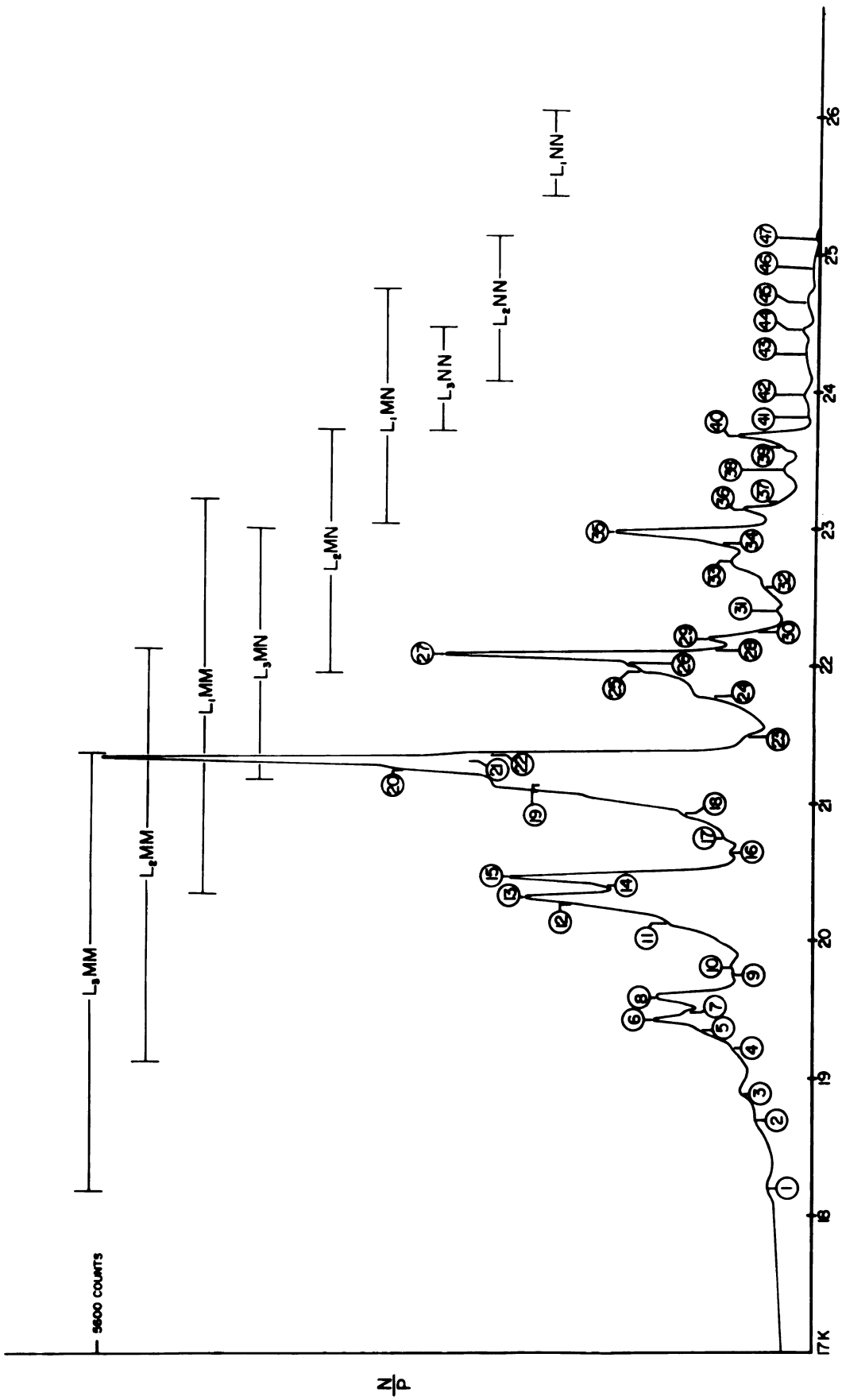

Figure 10. L-Auger Spectrum of In-113 as Derived From Sn-113.

TABLE II. Energies and Relative Intensities of the L-Auger Lines

Line No.	Trans.	Energy Calc. (ev)	Energy Meas. (ev)	Intensity $K\text{-}L_2L_3 = 1.00$	Comments
1.	$L_3\text{-}M_1M_1$	2047	2053	<0.10	
2.	$L_3\text{-}M_1M_2$	2173	2167	0.14	
3.	$L_3\text{-}M_1M_3$	2213	2211	0.24	signs of multiplet
4.	$L_3\text{-}M_2M_2$	2296	2290	0.30	
5.			2320		possibly D.E.L.
6.	$L_3\text{-}M_2M_3$	2336	2339	0.85	signs of multiplet
7.			2352		$L_3\text{-}M_2M_3$ I.C. satellite (?)
8.	$L_3\text{-}M_3M_3$	2373	2375	1.14	signs of multiplet
9.	$L_3\text{-}M_1M_4$ $L_2\text{-}M_1M_3$	2424 2420	2418	0.27	
10.	$L_3\text{-}M_1M_5$	2432	2431	0.48	
11.	$L_2\text{-}M_2M_2$	2504	2506	0.56	
12.	$L_2\text{-}M_2M_3$	2543	2542	0.77	
13.	$L_3\text{-}M_2M_5$	2558	2555	1.53	
14.	$L_2\text{-}M_3M_3$	2582	2577	0.88	
15.	$L_3\text{-}M_3M_5$	2595	2592	2.00	$L_3\text{-}M_3M_4$ contr.
16.	$L_2\text{-}M_1M_5$	2640	2639	0.40	$L_2\text{-}M_1M_4$ contr.
17.	$L_1\text{-}M_1M_2$	2680	2666	~0.10	(?)
18.	$L_1\text{-}M_1M_3$	2721	2712	~0.10	
19.	$L_2\text{-}M_2M_4$	2758	2763	2.09	$L_2\text{-}M_2M_5$ contr.
20.	$L_2\text{-}M_3M_4$ $L_3\text{-}M_4M_4$	2795 2800	2792	0.92	
21.	$L_3\text{-}M_4M_5$	2808	2808	4.18	$L_2\text{-}M_3M_5$ contr.

TABLE II. Cont'd

Line No.	Trans.	Energy Calc. (ev)	Energy Meas. (ev)	Intensity $K\text{-}L_2L_3 = 1.00$	Comments
22.	$L_3\text{-}M_5M_5$	2816	2821	1.90	
23.	$L_1\text{-}M_2M_3$	2843	2860	0.52	
	$L_1\text{-}M_3M_3$	2882			
24.	$L_3\text{-}M_2N_3$	2940	2939	0.39	$L_1\text{-}M_1M_5$ contr.
25.	$L_3\text{-}M_3N_3$	2978	2985	0.55	
26.	$L_3\text{-}M_2N_5$	3004	2999	0.30	
27.	$L_2\text{-}M_4M_5$	3016	3016	2.51	
28.	$L_2\text{-}M_5M_5$	3024	3028	0.32	
29.	$L_3\text{-}M_3N_5$	3042	3050	0.69	
30.	$L_1\text{-}M_2M_5$	3066	3063	0.19	
31.	$L_1\text{-}M_3M_5$	3103	3107	<0.10	(?)
32.	$L_2\text{-}M_2N_2$	3146	3150		
	$L_2\text{-}M_2N_3$	3148	↓	0.27	
	$L_3\text{-}M_5N_1$	3150	3160		
33.	$L_3\text{-}M_5N_3$	3199	3208	0.64	
	$L_2\text{-}M_2N_5$	3212			
34.	$L_2\text{-}M_3N_{4,5}$	3250	3246	0.26	
35.	$L_3\text{-}M_5N_{4,5}$	3262	3266	1.77	
36.	$L_1\text{-}M_4M_5$	3316	3316	0.50	
37.	$L_1\text{-}M_5M_5$	3324	3333	~ 0.10	
38.	$L_2\text{-}M_4N_{2,3}$	3398	3400	0.10	
	$L_2\text{-}M_5N_{2,3}$	3408			
39.	$L_1\text{-}M_2N_{2,3}$	3447	3448	<0.10	
40.	$L_2\text{-}M_5N_5$	3471	3471	0.60	$L_2\text{-}M_{4,5}N_{4,5}$ contr.

TABLE II. Cont'd

Line No.	Trans.	Energy Calc. (ev)	Energy Meas. (ev)	Intensity $K\text{-}L_2L_3 = 1.00$	Comments
41.	$L_1\text{-}M_2N_{4,5}$	3512	3512	<0.10	
42.	$L_1\text{-}M_3N_{4,5}$ $L_3\text{-}N_{2,3}N_{3,3}$		3560	~0.10	
43.	$L_3\text{-}N_{2,3}N_{4,5}$		3610 ↓ 3677	~0.10	
44.	$L_3\text{-}N_{4,5}N_{4,5}$ $L_1\text{-}M_5N_{2,3}$		3701	~0.10	
45.	$L_1\text{-}M_{4,5}N_{4,5}$ $L_2\text{-}N_{2,3}N_{2,3}$		3753 ↓ 3773	~0.10	
46.	$L_2\text{-}N_3N_5$	3836	3836	~0.10	
47.	$L_2\text{-}N_{4,5}N_{4,5}$		3904	<0.10	

sitions of the type $L_{1,2,3}$-$M_{1,2,3}M_{1,2,3}$; $L_{1,2,3}$-$M_{4,5}M_{4,5}$, respectively. For transitions of the type $L_{1,2,3}$-$M_{1,2,3}$ $M_{4,5}$ estimates were made for example by taking an average of L_1-M_1M_5 ($\Delta Z = 0.67$) and L_1-M_5M_1 ($\Delta Z = 0.55$). $\Delta Z = 1.0$ was used for all others. The energy calibration in the L-Auger region was based on the location of the K-L_2L_3 line which was assumed to have an energy of 20.144 kev based on a semiempirical table by Hornfeldt.[76] The energies in this table are estimated to be good to about 0.05%. A work function correction of 4 ev was also taken into account, due to the fact that the electron leaving the source will have to overcome a small electric field and loose an amount of energy roughly equal to the W.F. of the vacuum tank surface.

It must be remarked that the measured positions of a line were really center of gravity estimates of multiplets due to the fact that for Z = 49 we are removed from the pure j-j coupling limit. A crude line fitting effort, as hazardous as it is due to the previously mentioned reasons, was nevertheless used in a complementary way to aid in the identification and positioning of the lines. The estimated relative intensities are also given in Table II. A computer program assuming a gaussian shape with an exponential low energy tail was tried on some regions of the spectrum. This indicated that by means of parameters that were obtained

graphically, together with empirical data such as position of lines, estimated widths and heights, the standard deviation from an optimum fit was 20-30%. Thus, the column in Table II indicating the relative intensities should be construed as possessing errors of at least this order of magnitude and even worse for the very weak lines.

After the line fitting trials we feel that discrete energy losses (D.E.L.) were not prominent and may have manifested themselves only as gentle ripples on the low energy sides, particularly, in the low energy region of the spectrum. Subsequently they were ignored.

The existance of double vacancy effects which would arise when the L-Auger process follows the K-Auger process was investigated, insofar as the experimental data allowed it. The effect may be illustrated by considering a K-L_1L_3 transition which leaves the L shell doubly ionized, thus, effecting the screening of the electrons which are about to participate in a Auger transition, say, L_3-M_4M_5. To a first order approximation, if one can take into account the changes in screening correctly, the estimate of the energy shift of a double vacancy satellite line from its parent could be made purely on energetic grounds. The situation, however, is much more complex than in the usual Auger process since the initial state is comprised of two holes which can couple in some particular way and the matrix element

would look as follows,

$$\lambda = \text{CONST.} \left| \langle 2S_{1/2}\, 2P_{3/2}\, \underline{k} \left| \mathcal{H}_{ix} \right| 3d_{3/2}\, 3d_{5/2} \rangle \right|^2$$

Aside from the fact that this would introduce broadening of the double vacancy (multiplet) lines, it was not obvious how the energy shift could be estimated in an easy manner. A straight forward application of Slater's screening rules[77] gave a double vacancy shift of 16-18 ev to the low energy side of the most intense L_3-M_4M_5 line.

From the standpoint of intensity it was reasonable to expect noticeable double vacancy effects around, e.g., the L_3-M_4M_5 line (see Table I).* However, the search was impeded by the heavy overlaps of lines in that region, together with our inability to define the shape of the low energy side of lines (not to mention our lack of knowledge of their exact position). There seemed to be evidence in the form of unexplained residues in intensity around the low sides of lines, however, the

---

*The analogous process of x-ray satellites had been first reported by Siegbahn and Stenstrom[78] and was studied although not exhaustively in the 1930's. Recently Deodhar[79] and Hayasi[80] have given reviews of the origin and theory of x-ray satellite lines.

conclusion that the double vacancy effect was seen must remain somewhat speculative.

F. Conclusion

It has been shown that post-acceleration of magnetic spectrometer electron beams (with a gas counter as a detector) is a practical and successful method of studying very low energy beta-ray spectra.

The results of measurement of the L-Auger spectrum of In^{113} by means of a $\pi\sqrt{2}$ precision spectrometer indicate the very real feasibility of studying orbital electron capture ratios in this way. A sharper spectrum would be required which from the vantage point of this experiment appears possible. As it is the results of the relative intensities of the L-groups are too uncertain to attempt analysis of $L_1/L_2/L_3$, relative orbital capture probabilities. Although the ultimate goal of measuring these probabilities is not attained,* information about the L-Auger spectrum of a medium Z atom has been obtained, and constitutes the first attack of measuring very low energy Auger electrons with a precision spectrometer by means of a post-acceleration technique.

From the standpoint of technique, we believe

---

*A full discussion of this aspect of the problem must await the complete measurement and analysis of all of the electron spectra of the In^{113}-Sn^{113} system.

that thinner conducting source backings should be used in order to minimize backscattering. Carbon films would seem to offer the best solution for this. Source thickness effects could be further minimized if more stringent measures were taken in preventing the exposure of the source to air and vacuum pump oil. This could be managed by better vacuum systems (refrigerated baffles) both in the vacuum evaporator and the spectrometer itself. Accelerator produced sources also offer a new area by means of which high quality sources could be prepared.

From the standpoint of physical information gained the effective incremental charge ΔZ has been determined for the most prominent Auger transitions and the energies tabulated. Order of magnitude of relative intensities of the lines has been also determined. It has been shown that the spectrum exibited intermediate coupling features and that double vacancy effects probably exist.

REFERENCES

1. K. Siegbahn, Editor, α-β-γ-Ray Spectroscopy (North-Holland Publishing Co., 1965).

2. J. N. Bahcall, Phys. Rev. Letters, 9, 500 (1962).

3. J. N. Bahcall, Phys. Rev., 129, 2683 (1963).

4. J. N. Bahcall, Phys. Rev., 131, 1765 (1963).

5. R. E. Marshak, Phys. Rev., 61, 431 (1942).

6. H. Brysk and M. E. Rose, Revs. Modern Phys., 30, 1169 (1958).

7. S. Odiot and R. Daudel, J. Phys. Radium, 17, 60 (1956).

8. R. Bouchez and P. Depommier, Reports on Progress in Physics, 23, 395 (1960).

9. B. L. Robinson and R. W. Fink, Revs. Modern Phys., 32, 117 (1960).

10. L. J. Velinsky, Ph.D. Thesis, Michigan State University, (1964).

11. Nuclear Data Cards NRC-60-2-99, 100, 105, 106.

12. M. Schmorak, G. T. Emery and G. Scharf-Goldhaber, Phys. Rev., 124, 1186 (1961).

13. L. J. Velinsky, et al, to be published.

14. G. Backstrom, A. Backlin, N. E. Holmberg, Nucl. Instr. and Meth., 16, 199 (1962).

15. C. S. Cook, Nucleonics, 12, No. 2, 43 (1954).

16. M. S. Freedman, private communication.

17. R. O. Lane and D. J. Zaffarano, Phys. Rev., 94, 960 (1954).

18. M. S. Freedman, F. T. Porter, F. Wagner and P. P. Day, Phys. Rev., 108, 836 (1957).

19. H. A. Bethe, Handbuch der Physik (Verlag Julius Springer, Berlin, 1933), Bd. 24, p. 519.

20. C. H. Chang and C. S. Cook, Nucleonics, 10, No. 4, 24 (1952).

21. A. Juillard and M. A. Moussa, J. Phys. Rad., 19, 94 (1958).

22. H. M. Agnew and H. L. Anderson, Rev. Sci. Instr., 20, 869 (1949).

23. L. M. Langer and C. S. Cook, Rev. Sci. Instr., 19, 257 (1948).

24. D. K. Butt, Proc. Phys. Soc. Lond., 63A, 986 (1950).

25. G. Giroux and C. Geoffrion, Can. J. Phys., 34, 153 (1956).

26. W. T. Achor, Ph.D. Thesis, Vanderbilt University, (1958).

27. W. Mehlhorn, Z. Physik, 160, 247 (1960).

28. P. Erman and Z. Sujkowski, Ark. Fys., 20, 209 (1961).

29. Jose Sant'ana Dionisio, Ann. Phys., 9, 29 (1964).

30. J. S. Geiger, R. L. Graham and Janet S. Merrit, Nuclear Physics, 48, 97 (1963).

31. R. G. Albridge, private communication.

32. W. Mehlhorn and R. G. Albridge, Nuc. Instr. and Meth., 26, 37 (1964).

33. R. A. Parker, M.S. Thesis, Vanderbilt University, (1960).

34. R. C. Greenwood and E. Brannen, Phys. Rev., 122, 1849 (1961).

35. Willie E. Phillips and John I. Hopkins, Phys. Rev., 119, 1315 (1960).

36. S. B. Burson, H. A. Grench and L. C. Schmid, Phys. Rev., 115, 188 (1959).

37. W. T. Achor, W. E. Phillips, J. I. Hopkins and S. K. Haynes, Phys. Rev., 114, 137 (1959).

38. R. K. Girgis and R. Van Lieshout, Physica, 24, 672 (1958).

39. K. S. Bhatki, R. K. Gupka, S. Jha and B. K. Mandan, Il Nuovo Cimento Serie X, 6, 1461 (1957).

40. C. Manduchi, G. Nardelli, M. T. Russo-Manduchi and G. Zannoni, Il Nuovo Cimento Vol. XXXI, N. 6, 1380 (1964).

41. P. Avignon, Ann. Physique, 1, 10 (1956).
Y. Deschamps and P. Avignon, Compt. Rend. Ac. Sc. Paris, 236, 478 (1953).

42. C. D. Broyles, D. A. Thomas and S. K. Haynes, Phys. Rev., 89, 715 (1953).

43. R. G. Jung and M. L. Pool, Bull. Am. Phys. Soc., 1, 172 (1956).

44. M. A. Listengarten, Izvestia Akad. Nauk SSSR, (Physics) 24, 1050 (1960). (Transactions of the 10th Conference on Nuclear Spectroscopy.)

45. Jose Sant'ana Dionisio, Ann. Phys., 8, 747 (1963).

46. E. H. S. Burhop, The Auger Effect and other Radiationless Transitions (Cambridge University Press, London, 1952).

47. P. Auger, Comptes Rendus, 180, 65 (1925).

48. M. B. Stearns, The Spectroscopy of Mesic Atoms in Progress of Nuclear Physics, 6, 108 (1957).

49. D. Coster and R. De L. Kronig, Physica, 2, 13 (1935).

50. W. N. Asaad, Nuclear Physics, 63, 337 (1965).

51. E. J. Callan, Rev. Mod. Phys., 35, 524 (1963).

52. W. N. Asaad and E. H. S. Burhop, Proc. Phys. Soc., 71, 369 (1958).

53. E. J. Callan, Phys. Rev., 124, 793 (1961).

54. W. N. Asaad, Proc. Roy. Soc., 249, 555 (1959).

55. W. N. Asaad, Nuclear Physics, 44, 399 (1963).

56. M. A. Listengarten, Izvestia Akad. Nauk SSSR, (Physics) 25, 792 (1961).

57. M. A. Listengarten, Izvestia Akad. Nauk SSSR, (Physics) 26, 182 (1962).

58. R. A. Rubenstein, Ph.D. Thesis, University of Illinois, (1955).

59. Z. Sujkowski and O. Melin, Arkiv Fysik, 20, 193 (1961).

60. G. Albouy and M. Valaderes, Comptes Rendus, 250, 2877 (1960).

61. J. C. Nall, Q. L. Baird and S. K. Haynes, Phys. Rev., 118, 1278 (1960).

62. J. Burde and S. G. Cohen, Phys. Rev., 104, 1085 (1956).

63. K. Risch, Z. Phys., 150, 87 (1958).

64. C. Geoffrion and G. Nadeau, Can. J. Phys., 35, 1284 (1957).

65. R. G. Albridge and J. M. Hollander, Nuclear Physics, 27, 554 (1961).

66. Z. Sujkowski and H. Slatis, Arkiv Fysik, 14, 101 (1958).

67. I. Bergstrom, F. Brown, J. A. Davies, J. S. Geiger, R. L. Graham and R. Kelly, Nuclear Instruments and Methods, 21, 249 (1963).

68. Jerry Lerner, Argonne National Laboratory, private communication.

69. K. Risch, Z. Phys. 159, 89 (1960).

70. E. G. Ramberg and F. K. Richtmeyer, Phys. Rev., 51, 913 (1937).

71. F. K. Richtmeyer and E. G. Ramberg, Phys. Rev., 51, 925 (1937).

72. R. L. Graham, I. Bergstrom and F. Brown, Nuclear Physics, 39, 107 (1962).

73. C. Nordling, E. Sokolowski and K. Siegbahn, Phys. Rev., 105, 1676 (1957).

74. D. Bohm and D. Pines, Phys. Rev., 92, 609 (1953).

75. I. Bergstrom and R. D. Hill, Arkiv Fysik, 8, 21 (1954).

76. O. Hornfeldt, Arkiv Fysik, 23, 235 (1963).

77. A. H. Wapstra, G. J. Nijgh and R. van Lieshout, Nuclear Spectroscopy Tables (North-Holland Publishing Co., Amsterdam, 1959).

78. M. Siegbahn and W. Stenstrom, Physik. Zeit., 17, 48, 318 (1916).

79. G. B. Deodhar, Proc. Nat. Acad. Sci. India A, 32, 320 (1962).

80. Takesi Hayasi, Sci. Rep. Tohoku Univ. First Ser. (Japan) 46, No. 2, 82 (1960).